IOP Publishing New J. Phys. 26 (2024) 053032 https://doi.org/10.1088/1367-2630/ad4818

New Journal of Physics
The open access journal at the forefront of physics

Deutsche Physikalische Gesellschaft DPG
IOP Institute of Physics

Published in partnership with: Deutsche Physikalische Gesellschaft and the Institute of Physics

OPEN ACCESS

RECEIVED
5 December 2023

REVISED
19 April 2024

ACCEPTED FOR PUBLICATION
7 May 2024

PUBLISHED
22 May 2024

PAPER

Quantum–classical correspondence in spin–boson equilibrium states at arbitrary coupling

F Cerisola[1,2,*], **M Berritta**[1], **S Scali**[1], **S A R Horsley**[1], **J D Cresser**[1,3,4] **and J Anders**[1,5,*]

[1] Department of Physics and Astronomy, University of Exeter, Stocker Road, Exeter EX4 4QL, United Kingdom
[2] Department of Engineering Science, University of Oxford, Oxford OX1 3PJ, United Kingdom
[3] School of Physics and Astronomy, University of Glasgow, Glasgow G12 8QQ, United Kingdom
[4] Department of Physics and Astronomy, Macquarie University, Sydney, NSW 2109, Australia
[5] Institut für Physik und Astronomie, University of Potsdam, 14476 Potsdam, Germany
[*] Authors to whom any correspondence should be addressed.

E-mail: f.cerisola@exeter.ac.uk and janet@qipc.org

Keywords: quantum thermodynamics, open quantum systems, spin–boson model, mean force state, quantum–classical correspondence, strong coupling thermodynamics

Abstract

The equilibrium properties of nanoscale systems can deviate significantly from standard thermodynamics due to their coupling to an environment. We investigate this here for the θ-angled spin–boson model, where we first derive a compact and general form of the classical equilibrium state including environmental corrections to all orders. Secondly, for the quantum spin–boson model we prove, by carefully taking a large spin limit, that Bohr's quantum–classical correspondence persists at all coupling strengths. This shows, for the first time, the validity of the quantum–classical correspondence for an open system and gives insight into the regimes where the quantum system is well-approximated by a classical one. Finally, we provide the first classification of the coupling parameter regimes for the spin–boson model, from weak to ultrastrong, both for the quantum case and the classical setting. Our results shed light on the interplay of quantum and mean force corrections in equilibrium states of the spin–boson model, and will help draw the quantum to classical boundary in a range of fields, such as magnetism and exciton dynamics.

Bohr's correspondence principle [1] played an essential role in the early development of quantum mechanics. Since then, a variety of interpretations and applications of the correspondence principle have been explored [2–9]. One form asks if the statistical properties of a quantum system approach those of its classical counterpart in the limit of large quantum numbers [4, 5]. This question was answered affirmatively by Millard and Leff, and Lieb for a quantum spin system [2, 3]. They proved that the system's thermodynamic partition function Z_S^{qu} associated with the Gibbs state, converges to the corresponding classical partition function Z_S^{cl}, in the limit of large spins. Such correspondence gives insight into the conditions for a quantum thermodynamic system to be well-approximated by its classical counterpart [8, 9]. While Z_S^{qu} is computationally tough to evaluate for many systems, Z_S^{cl} offers tractable expressions with which thermodynamic properties, such as free energies, susceptibilities and correlation functions, can readily be computed [2, 3]. Similarly, many dynamical approaches solve a classical problem rather than the much harder quantum problem. For example, sophisticated atomistic simulations of the magnetisation dynamics in magnetic materials [10–13] solve the evolution of millions of interacting classical spins. A corresponding quantum simulation [14] would require no less than a full–blown quantum computer as its hardware.

Meanwhile, in the field of quantum thermodynamics, extensive progress has recently been made in constructing a comprehensive framework of 'strong coupling thermodynamics' for classical [15–20] and quantum [21–31] systems. This framework extends standard thermodynamic relations to systems whose coupling to a thermal environment can not be neglected. The equilibrium state is then no longer the quantum or classical Gibbs state, but must be replaced with the environment-corrected mean force (Gibbs) state [30–32]. These modifications bring into question the validity of the correspondence principle when the

environment-coupling is no longer negligible. Mathematically, the challenge is that in addition to tracing over the system, one must also evaluate the trace over the environment.

Strong coupling contributions are present for both classical and quantum systems. However, a quantitative characterisation of the difference between these two predictions, in various coupling regimes, is missing. For example, apart from temperature, what are the parameters controlling the deviations between the quantum and classical spin expectation values? And how strong does the environmental coupling need to be for the spin–boson model to be well-described by weak or ultrastrong coupling approximations? In this paper, we answer these questions for the particular case of a spin S_0 coupled to a one-dimensional bosonic environment such that both dephasing and detuning can occur (θ-angled spin–boson model).

1. Setting

This generalised version of the spin–boson model [33, 34] describes a vast range of physical contexts, including excitation energy transfer processes in molecular aggregates described by the Frenkel exciton Hamiltonian [35–41], the electronic occupation of a double quantum dot whose electronic dipole moment couples to the substrate phonons in a semi-conductor [42], an electronic, nuclear or effective spin exposed to a magnetic field and interacting with an (anisotropic) phononic, electronic or magnonic environment [43–47], and a plethora of other aspects of quantum dots, ultracold atomic impurities, and superconducting circuits [48–51]. In all these contexts, an effective 'spin' $\mathbf{S}$ interacts with an environment, where $\mathbf{S}$ is a vector of operators (with units of angular momentum) whose components fulfil the angular momentum commutation relations $[S_j, S_k] = i\hbar\sum_l \epsilon_{jkl} S_l$ with $j,k,l \in \{x,y,z\}$. We will consider spins of any length S_0, i.e. $\mathbf{S}^2 = S_0(S_0+\hbar)\mathbf{1}$. The system Hamiltonian is

$$H_{\mathrm{S}} = -\omega_L S_z, \tag{1}$$

where the system energy level spacing is $\hbar\omega_{\mathrm{L}} > 0$ and the energy axis is in the $-z$-direction without loss of generality. For a double quantum dot, the frequency ω_{L} is determined by the energetic detuning and the tunneling between the dots [42]. For an electron spin with $S_0 = \hbar/2$, the energy gap is set by a gyromagnetic ratio γ and an external magnetic field $\mathbf{B}_{\mathrm{ext}} = -B_{\mathrm{ext}}\hat{\mathbf{z}}$, such that $\omega_{\mathrm{L}} = \gamma B_{\mathrm{ext}}$ is the Larmor frequency.

The spin system is in contact with a bosonic reservoir, which is responsible for the dissipation and equilibration of the system. Typically, this environment will consist of phononic modes or an electromagnetic field [31, 52]. The bare Hamiltonian of the reservoir is

$$H_{\mathrm{R}} = \frac{1}{2}\int_0^\infty \mathrm{d}\omega \left(P_\omega^2 + \omega^2 X_\omega^2\right), \tag{2}$$

where X_ω and P_ω are the position and momentum operators of the reservoir mode at frequency ω which satisfy the canonical commutation relations $[X_\omega, P_{\omega'}] = i\hbar\delta(\omega-\omega')$. With the identifications made in (1) and (2), the system-reservoir Hamiltonian is

$$H_{\mathrm{tot}} = H_{\mathrm{S}} + H_{\mathrm{R}} + H_{\mathrm{int}}, \tag{3}$$

which contains a system-reservoir coupling H_{int}. Physically, the coupling can often be approximated to be linear in the canonical reservoir operators [31], and is then modelled as [42, 52, 53]

$$H_{\mathrm{int}} = S_\theta \int_0^\infty \mathrm{d}\omega\, C_\omega X_\omega, \tag{4}$$

where the coupling function C_ω determines the interaction strength between the system and each reservoir mode ω. C_ω is related to the reservoir spectral density J_ω via $J_\omega = C_\omega^2/(2\omega)$. It is important to note that the coupling is via the spin (component) operator $S_\theta = S_z\cos\theta - S_x\sin\theta$ which is at an angle θ with respect to the system's bare energy axis, see figure 1. For example, for a double quantum dot [42], the angle θ is determined by the ratio of detuning and tunnelling parameters.

In what follows, we will need an integrated form of the spectral density, namely

$$Q = \int_0^\infty \mathrm{d}\omega\, \frac{J_\omega}{\omega} = \int_0^\infty \mathrm{d}\omega\, \frac{C_\omega^2}{2\omega^2}. \tag{5}$$

This quantity is a measure of the strength of the system–environment coupling and it is sometimes called 'reorganization energy' [32, 54–56]. The analytical results discussed below are valid for arbitrary coupling functions C_ω (or reorganisation energies Q). The plots assume Lorentzians

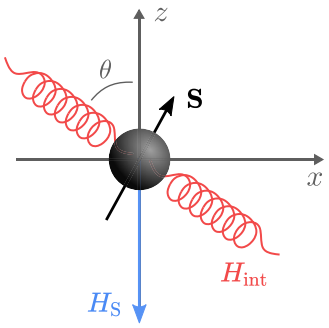

Figure 1. Illustration of bare and interaction energy axes. A spin operator (vector) **S** with system Hamiltonian H_S with energy axis in the $-z$-direction is coupled in θ-direction to a harmonic environment via H_{int}.

$J_\omega = (2\Gamma Q/\pi)\omega_0^2\omega/((\omega_0^2-\omega^2)^2+\Gamma^2\omega^2)$, where ω_0 is the resonant frequency of the Lorentzian [43] and Γ the peak width.

We will model H_{tot} (equation (3)) either fully quantum mechanically as detailed above, or fully classically. To obtain the classical case, the spin **S** operator will be replaced by a three-dimensional vector of length S_0, and the reservoir operators X_ω and P_ω will be replaced by classical phase–space coordinates. Below, we evaluate the spin's so-called mean force (Gibbs) states, CMF and QMF, for the classical and quantum case, respectively. The mean force approach postulates [31] that the equilibrium state of a system in contact with a reservoir at temperature T is the mean force (MF) state, defined as

$$\tau_{MF} := \mathrm{tr}_R\left[\tau_{tot}\right] = \mathrm{tr}_R\left[\frac{e^{-\beta H_{tot}}}{Z_{tot}}\right]. \tag{6}$$

That is, τ_{MF} is the reduced system state of the global Gibbs state τ_{tot}, where $\beta = 1/k_B T$ is the inverse temperature with k_B the Boltzmann constant, and Z_{tot} is the global partition function. Quantum mechanically, tr_R stands for the operator trace over the reservoir space while classically, 'tracing' is done by integrating over the reservoir degrees of freedom. Further detail on classical and quantum tracing for the spin and the reservoir, respectively, is given in appendix A.

While the formal definition of τ_{MF} is deceptively simple, carrying out the trace over the reservoir—to obtain a quantum expression of τ_{MF} in terms of system operators alone—is notoriously difficult. Often, expansions for weak coupling are made [21, 42]. For a general quantum system (i.e. not necessarily a spin), an expression of τ_{MF} has recently been derived in this limit [32]. Furthermore, recent progress has been made on expressions of the quantum τ_{MF} in the limit of ultrastrong coupling [32], and for large but finite coupling [30, 31, 58]. Moreover, high temperature expansions have been derived that are also valid at intermediate coupling strengths [41]. However, the low and intermediate temperature form of the quantum τ_{MF} for intermediate coupling is not known, neither in general nor for the θ–angled spin boson model.

2. Classical MF state at arbitrary coupling

In contrast, here we establish that the analogous problem of a *classical* spin vector of arbitrary length S_0, coupled to a harmonic reservoir via equation (4), is tractable for arbitrary coupling function C_ω and arbitrary temperature. By carrying out the (classical) partial trace over the reservoir, i.e. $\mathrm{tr}_R^{cl}[\tau_{tot}]$ see appendix C, we uncover a rather compact expression for the spin's CMF state τ_{MF} and the CMF partition function $\tilde{Z}_S^{cl}$:

$$\tau_{MF} = \frac{e^{-\beta\left(H_S - QS_\theta^2\right)}}{\tilde{Z}_S^{cl}},$$
$$\text{with} \quad \tilde{Z}_S^{cl} = \mathrm{tr}_S^{cl}\left[e^{-\beta\left(H_S - QS_\theta^2\right)}\right], \tag{7}$$

where the mean force nature of the partition function is indicated with a $\tilde{}$. The state τ_{MF} clearly differs from the standard Gibbs state by the presence of the reorganisation energy term $-QS_\theta^2$. The quadratic dependence on S_θ changes the character of the distribution, from a standard exponential to an exponential with a positive quadratic term, altering significantly the state whenever the system–reservoir coupling is non-negligible.

Throughout this article, we will consider that the MF state is the equilibrium state reached by a system in contact with a thermal bath. While this is widely thought to be the case, some open questions remain about

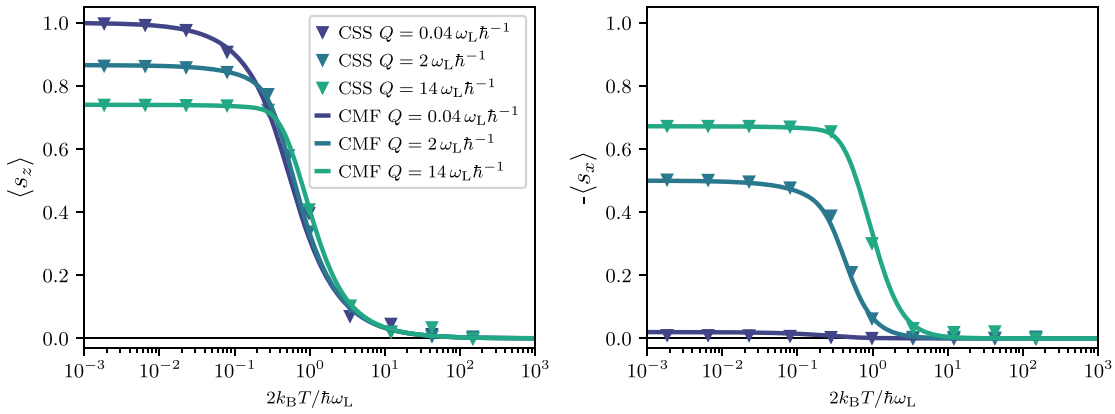

Figure 2. Classical mean force and steady–state spin expectation values. Normalised expectation values of the classical spin components $\langle s_z \rangle$ (left) and $\langle s_x \rangle$ (right) as a function of temperature. These are obtained with: (CSS) the long time average of the dynamical evolution of the spin, $\langle s_k \rangle = \langle S_k \rangle_{\mathrm{CSS}}/S_0$; and (CMF) the classical MF state (equation (7)), $\langle s_k \rangle = \langle S_k \rangle_{\mathrm{MF}}/S_0$. These are shown for three different coupling strengths $Q = 0.04\,\omega_L\hbar^{-1}, 2\,\omega_L\hbar^{-1}, 14\,\omega_L\hbar^{-1}$, that range from the weak to the ultrastrong coupling regime. In all three cases, we see that the MF predictions are fully consistent with the results of the dynamics. All plots are for Lorentzian coupling with $\omega_0 = 7\omega_L$, $\Gamma = 5\omega_L$, and coupling angle $\theta = 45°$. The temperature scale shown corresponds to a spin $S_0 = \hbar/2$. The dynamical simulations where numerically computed using SpiDy.jl [57], a library for the simulation of the non-Markovian stochastic dynamics of classical spins strongly coupled to the environment.

formal proofs showing the convergence of the dynamics towards the steady state predicted by the MF state [24–26, 31, 42, 59–64]. For example, for quantum systems, this convergence has only been proven in the weak [21] and ultrastrong limits [30], while for intermediate coupling strengths there is numerical evidence for the validity of the MF state [34]. Here, we numerically verify the convergence of the dynamics towards the MF state for the case of the classical spin at arbitrary coupling strength. This is possible thanks to the numerical method proposed in [43], see also the optimised implementation in the SpiDy.jl package [57]. For the classical spin, figure 2 shows the long time average of the spin components once the dynamics has reached steady state (CSS, triangles), together with the expectation values predicted by the static MF state (CMF, solid lines), for a wide range of coupling strengths going from weak to strong coupling (see also section 4 for the first full characterisation of the different coupling strength regimes). We find that both predictions are in excellent agreement, providing strong evidence for the convergence of the dynamics towards the MF. The compact expression (7) for the CMF state, as well as the numerical verification that the dynamical steady state matches the CMF state, are the first result of this paper.

3. Quantum–classical correspondence

We now demonstrate that the quantum *mean force* partition function $\tilde{Z}_S^{\mathrm{qu}}$, which includes arbitrarily large corrections due to the spin's coupling to the reservoir, converges to the classical one, $\tilde{Z}_S^{\mathrm{cl}}$ in equation (7).

A well-known classical limit of a quantum spin is to increase the quantum spin's length, $S_0 \to \infty$. This is because, when S_0 increases, the quantised angular momentum level spacing relative to S_0 decreases, approaching a continuum of states that can be described in terms of a classical vector [1]. Taking the large spin limit for a spin-S_0 system can be achieved following an approach used by Fisher when treating an uncoupled spin with Hamiltonian H_S [65]. This involves introducing a rescaling of the spin operators via $s_j = S_j/S_0$ so that the commutation rule becomes $[s_j, s_k] = i\hbar\,\epsilon_{jkl}\,s_l/S_0$. Hence, in the limit of $S_0 \to \infty$, the scaled operators will commute, so in that regard they can be considered as classical quantities [65]. Millard & Leff [2] take this further and prove, for any spin Hamiltonian H in the spin Hilbert space $\mathcal{H}_S$, the identity

$$\lim_{S_0\to\infty} \frac{\hbar}{2S_0+\hbar}\,\mathrm{tr}_S^{\mathrm{qu}}\left[\mathrm{e}^{-\beta H}\right] = \lim_{S_0\to\infty} \frac{1}{4\pi}\int_0^{2\pi}\mathrm{d}\varphi\int_0^{\pi}\mathrm{d}\vartheta\,\sin\vartheta\,\mathrm{e}^{-\beta H(S_0,\vartheta,\varphi)}, \tag{8}$$

provided the limit on the right hand side exists. Here $H(S_0, \vartheta, \varphi)$ is the classical spin-S_0 Hamiltonian, where the spin-vector $\mathbf{S}$ is parametrised by two angles, φ and ϑ, such that $S_x = S_0 \sin\vartheta\cos\varphi$, $S_y = S_0 \sin\vartheta \sin\varphi$ and $S_z = S_0\cos\vartheta$. The factor of $\hbar/(2S_0 + \hbar)$ guarantees that the sides of (8) are equal for $\beta = 0$. For a fixed value of S_0, this pre-factor is unimportant for thermodynamic expectation values as it immediately cancels in any calculation of expectation values, i.e. for a quantum system, the expressions $\frac{\hbar}{2S_0+\hbar} Z_S^{\mathrm{qu}}(\beta, S_0)$ and $Z_S^{\mathrm{qu}}(\beta, S_0)$ give the same expectation values. Equation (8) was further confirmed by Lieb who provides a rigorous argument based on the properties of spin-coherent states [3].

Note, though, if one simply takes the $S_0 \to \infty$ limit in (8), with H being the system Hamiltonian $H_S \propto S_0$, that would have the same effect as sending $\beta \to \infty$; namely, all population will go to the ground state. Instead, maintaining a non-trivial temperature dependence after taking the S_0-limit requires a further rescaling step. One approach involves a rescaling of the physical parameters of the Hamiltonian H, as followed, e.g. by Fisher [65]. A second approach is to rescale the inverse temperature via $\beta S_0 = \beta'$, and take the limit $S_0 \to \infty$ with β' held fixed. This is the limit we will take here. The effect of this constrained limit can readily be seen for the thermal states of the uncoupled classical or quantum spin. The classical partition function $Z_S^{\rm cl}(\beta S_0) = \sinh(\beta S_0 \omega_L)/\beta S_0 \omega_L$ is left invariant because β and S_0 always appear together in $Z_S^{\rm cl}$. In contrast, the quantum partition function $Z_S^{\rm qu}(\beta, S_0) = \sinh(\beta(S_0 + \hbar/2)\omega_L)/\sinh(\beta\hbar\omega_L/2)$ is altered in the constrained limit, since $Z_S^{\rm qu}$ separately depends on β and S_0. Equation (8) then expresses the convergence of the partition functions [2, 3, 65], i.e. $\frac{\hbar}{2S_0+\hbar} Z_S^{\rm qu}(\beta, S_0) \to Z_S^{\rm cl}(\beta S_0)$.

We now take a step further and extend this result to the case of a spin *coupled to a reservoir*. The first step is to consider that the relevant Hilbert space is now the tensor product space of spin and reservoir degrees of freedom, $\mathcal{H}_S \otimes \mathcal{H}_B$. It was argued by Lieb [3] that (8) remains valid in this case, i.e. even when $H \in \mathcal{H}_S \otimes \mathcal{H}_B$. This means we can replace H in (8) with our $H_{\rm tot}$. But note that the trace is still only over the system Hilbert space $\mathcal{H}_S$. Thus, formally one obtains an operator valued identity for operators on $\mathcal{H}_B$. The second step is then to evaluate the trace over the reservoir degrees of freedom. To do so, we start by writing the total unnormalised Gibbs state as

$$\mathrm{e}^{-\beta H_{\rm tot}} = \exp\left[-\beta'\left(-\omega_L s_z + \frac{H_{\rm R}}{S_0} + s_\theta \int_0^\infty \mathrm{d}\omega\, C_\omega X_\omega\right)\right], \tag{9}$$

with the rescaled inverse temperature $\beta' = \beta S_0$. Since β' is constant as the limit $S_0 \to \infty$ is taken, doing so rescales the spin operators, as required. But it also rescales $H_{\rm R}$ to $h_{\rm R} = H_{\rm R}/S_0$, which can be expressed in terms of rescaled reservoir operators, p_ω and x_ω where $p_\omega = P_\omega/\sqrt{S_0}$ and $x_\omega = X_\omega/\sqrt{S_0}$. The commutation relations are then $[x_\omega, p_{\omega'}] = i\hbar\,\delta(\omega - \omega')/S_0$, so in the limit of $S_0 \to \infty$, these two operators commute [66]. Thus, the classical limit of the spin induces a limit for the reservoir. That is, the quantum nature of the reservoir is inevitably stripped away, so that the result eventually obtained is that of a classical spin coupled to a classical reservoir.

Written in terms of these rescaled reservoir operators, one now has,

$$\mathrm{e}^{-\beta H_{\rm tot}} = \exp\left[-\beta'\left(-\omega_L s_z + h_R + s_\theta \int_0^\infty \mathrm{d}\omega\, C_\omega \sqrt{S_0}\, x_\omega\right)\right]. \tag{10}$$

If one were to naively take the S_0-limit, then the interaction term dominates and the dependence on the bare system energy $-\omega_L s_z$ drops out. To explore a non-trivial limit, where the relative energy scale of the bare and interaction Hamiltonians are kept the same throughout the S_0 limit, we now choose the scaling $C_\omega \propto 1/\sqrt{S_0}$ of the coupling function C_ω with spin-length S_0 (we will comment on other scaling choices below). The reorgansiation energy (5) then scales with S_0 as

$$Q = \alpha \frac{\omega_{\rm L}}{S_0}, \tag{11}$$

where α is a unit-free constant independent of S_0 and β. The combined scaling of Q with S_0 (equation (11)), and the rescaling of the inverse temperature, $\beta S_0 = \beta' = \text{const}$, then leaves the CMF state (7) invariant under variation of S_0.

Crucially, the QMF state defined by equation (6) will not be invariant under variation of S_0. Returning to the unnormalised total Gibbs state (10), taking the quantum trace over the spin, and using equation (8), one obtains an identity that still contains the bath operators in contrast to the uncoupled spin. Finally taking the quantum trace over the reservoir on both sides, one finds, see appendix D, the quantum–classical correspondence for the open spin's mean force partition functions:

$$\lim_{S_0 \to \infty} \frac{\hbar}{2S_0 + \hbar} \tilde{Z}_S^{\rm qu}(\beta, S_0, \alpha) = \tilde{Z}_S^{\rm cl}(\beta S_0, \alpha). \tag{12}$$

Here it was used that the total quantum partition function, $Z_{\rm SR}^{\rm qu}(\beta, S_0, \alpha)$, divided by the bare quantum reservoir partition function, $Z_{\rm R}^{\rm qu}(\beta)$, is the quantum mean force partition function, $\tilde{Z}_S^{\rm qu}(\beta, S_0, \alpha)$, i.e. $Z_{\rm SR}^{\rm qu}(\beta, S_0, \alpha)/Z_{\rm R}^{\rm qu}(\beta) = \tilde{Z}_S^{\rm qu}(\beta, S_0, \alpha)$ [67, 68]. In contrast to the quantum–classical correspondence established by Millard & Leff, and Lieb, for the standard Gibbs state partition functions, there now is a dependence on the spin-environment coupling strength α. Proving the quantum–classical correspondence (12) for the spin–boson model, valid at all coupling strengths, is the second result of the

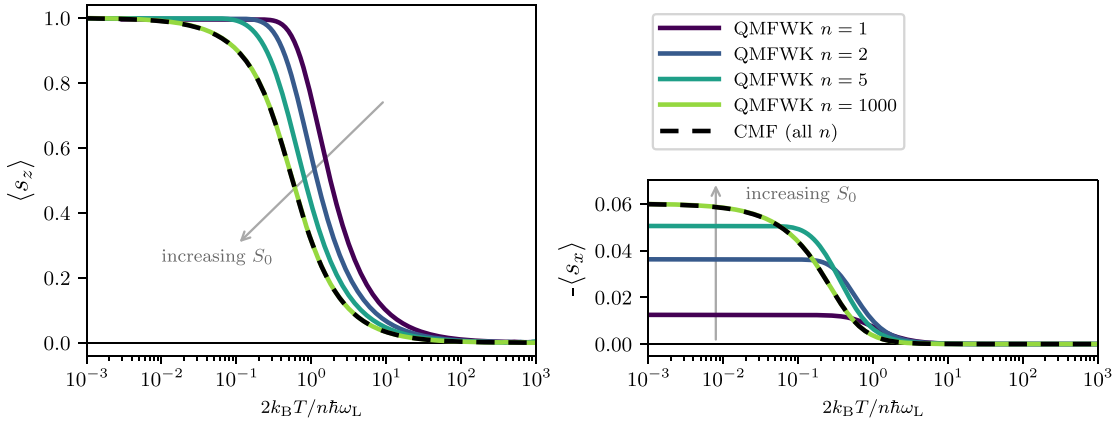

Figure 3. Classical and quantum mean force spin components. Normalised expectation values of the spin components $\langle s_z \rangle$ (left) and $\langle s_x \rangle$ (right) obtained with: (QMFWK) the quantum MF partition function $\tilde{Z}_S^{qu}$ in the weak coupling limit for a spin of length $S_0 = n\hbar/2$ ($n = 1, 2, 5, 100$); (CMF) the classical MF partition function $\tilde{Z}_S^{cl}$ given in (7). As the length S_0 of the quantum spin is increased, the quantum mean force prediction QMFWK converges to that corresponding to the CMF state. Non-zero s_x (right) indicate 'coherences' with respect to the system's bare energy axis (z). These arise entirely due to the spin-reservoir interaction. Such coherences have been discussed for the quantum case [42]. Here we find that they also arise in the classical CMF. All plots are for a weak coupling strength, $\alpha = 0.06$, and $\theta = \pi/4$.

paper. To our knowledge, this is the first time that such correspondence has been established for an *open* quantum system.

The above quantum–classical correspondence was derived assuming a constant ratio between bare and interaction energy, i.e. $C_\omega \propto 1/\sqrt{S_0}$. Different scaling choices also show a quantum–classical correspondence—but a much more trivial one where the dependence on α drops out. To see this, consider scalings of the form $C_\omega \propto 1/\sqrt{S_0^p}$, first for $p > 1$. Taking again the constrained large spin limit, as detailed in appendix D, the bare energy will stay constant while the interaction term then decays as $1/S_0^{p-1}$. This immediately results in recovering the CMF partition function but in the regime where the spin is negligibly coupled to a reservoir, i.e. $\frac{\hbar}{2S_0+\hbar}\tilde{Z}_S^{qu}(\beta, S_0, \alpha) \to \tilde{Z}_S^{cl}(\beta S_0, 0) \equiv Z_S^{cl}(\beta S_0)$. Correspondingly for $0 \leqslant p < 1$, the interaction term will grow when taking the large spin limit. The regime where the interaction is the dominant term is called the 'ultrastrong' limit [32], see also section 4 below. It is known that the QMF partition function's dependence on α drops out in this limit and a specific expression is recovered [32]. Besides, as we show in appendix G, at ultrastrong coupling, the quantum and classical mean force partition functions $\tilde{Z}_{S,US}^{qu}(\beta, S_0)$ and $\tilde{Z}_{S,US}^{cl}(\beta S_0)$ are identical. Hence, one has the trivial quantum–classical correspondence $\frac{\hbar}{2S_0+\hbar}\tilde{Z}_S^{qu}(\beta, S_0, \alpha) \to \tilde{Z}_{S,US}^{cl}(\beta S_0)$ for the quantum and classical MF partition functions.

We finally remark that, in the above proof, it was assumed that α is independent of β. Physically this is not entirely accurate because the coupling C_ω is usually a function of temperature [69], albeit often a rather weak one. For the limiting process leading to (12) to apply, a weak dependence on β would need to be compensated by an equally weak additional dependence of Q on S_0.

To visually illustrate the quantum to classical convergence, we choose a weak coupling strength, $\alpha = 0.06$, for which an analytical form of the quantum $\tilde{Z}_S^{qu}$ is known [32]. Mean force spin component expectation values $\langle s_k \rangle = \langle S_k \rangle_{MF}/S_0$ for $k = x, z$ can then readily be computed from the partition functions $\tilde{Z}_S^{qu}$ and $\tilde{Z}_S^{cl}$, respectively, see appendix B. Figure 3 shows $\langle s_z \rangle$ and $\langle s_x \rangle$ for various spin lengths, $S_0 = n\hbar/2$ with $n = 1, 2, 5, 1000$ for the quantum case (QMFWK, purple to green) and the classical case (CMF, dashed black). Note, that the x-axis is a correspondingly rescaled temperature, $2k_B T/n\hbar\omega_L$, a scaling under which the CMF remains invariant. The numerical results illustrate that the quantum $\langle s_z \rangle$ and $\langle s_x \rangle$ change with spin length $S_0 = n\hbar/2$, and indeed converge to the classical prediction in the large spin limit, $n \to \infty$.

4. Coupling regimes

Finally, we now classify the interaction strength necessary for the spin–boson model to fall in various coupling regimes, from ultra-weak to ultra-strong. To quantify the relative strength of coupling we use the dimensionless parameter

$$\zeta = \frac{QS_0}{\omega_L}, \tag{13}$$

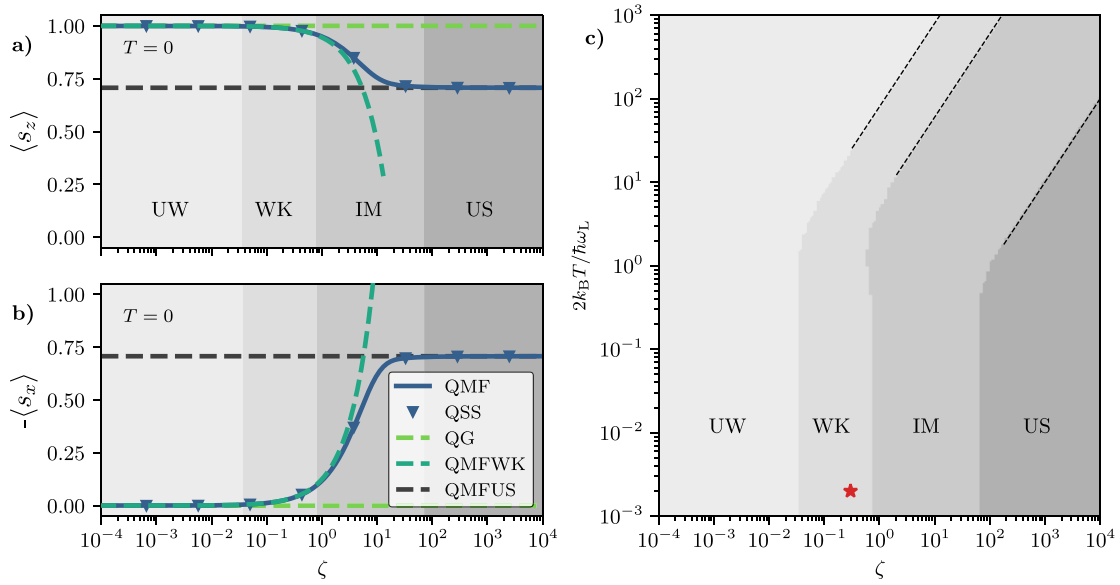

Figure 4. Quantum coupling regimes at $T = 0$ and $T > 0$. Panels **(a)** and **(b)**: Spin expectation values $\langle s_z \rangle$ and $-\langle s_x \rangle$ for the MF state (6) at $T = 0$ for the total Hamiltonian (3) with $S_0 = \hbar/2$, $\theta = \pi/4$ and different coupling strengths as quantified by the dimensionless parameter ζ, see (13). We identify four coupling regimes for the numerically exact QMF state (solid dark blue): Ultraweak coupling (UW), where the spin expectation values are consistent with the Gibbs state (QG, dashed light green); Weak coupling (WK), where the expectation values are well approximated by a second order expansion in ζ (QMFWK, dashed turquoise) [42]; Ultrastrong coupling (US), where the asymptotic limit of infinitely strong coupling $\zeta \to \infty$ is valid (QMFUS, dashed grey) [32], and Intermediate coupling (IM) where the QMF state is not approximated by any known analytical expression. The dynamical steady state of the quantum spin (QSS, dark blue triangles) is also computed using the reaction coordinate technique [71–74]. Excellent agreement between the QSS and the QMF prediction is seen for all ζ. Panel **c)**: Coupling regimes as a function of temperature T and coupling strength ζ. With increasing temperature, the boundaries shift towards higher coupling ζ. At large temperatures, all three boundaries follow a linear relation $T \propto \zeta$ (dashed lines).

which is the ratio of interaction and bare energy terms, see also equation (7). For scaling (11) one has $\zeta = \alpha$. It's important to note that temperature sets another scale in this problem: as we will see, higher temperatures will allow higher coupling values ζ to still fall within the 'weak' coupling regime [32, 70]. Thus, we will first characterise various coupling regimes at $T = 0$ K, where the coupling has the most significant effect on the system equilibrium state, and then proceed to study finite temperatures.

Figures 4(a) and (b) show the spin components $\langle s_z \rangle$ and $\langle s_x \rangle$ in the quantum MF state (QMF, solid dark blue) at $T = 0$ K. These expressions are evaluated numerically using the reaction coordinate method [71–74] see appendix E, for $S_0 = \hbar/2$ and angle $\theta = \pi/4$. Also shown are the spin components for the quantum Gibbs state (QG, dashed green), and for the analytically known quantum MF state in the weak coupling limit (QMFWK, dashed turquoise) and the ultrastrong coupling limit (QMFUS, dashed grey) [32].

By comparing the analytical results (dashed lines) to the numerically exact result (solid line), and requiring the relative error to be at most $4 \cdot 10^{-3}$, we can clearly identify four regimes: For $\zeta < 4 \cdot 10^{-2}$, equilibrium is well-described by the quantum Gibbs state and this parameter regime can thus can be considered as ultraweak coupling (UW) [31]. For $4 \cdot 10^{-2} \leqslant \zeta < 8 \cdot 10^{-1}$, equilibrium is well-described by the weak coupling state QMFWK, which includes second order coupling corrections [32]. Thus, this regime is identified as the weak coupling regime (WK). At the other extreme, for $7 \cdot 10^{1} \leqslant \zeta$, the equilibrium state converges to the ultrastrong coupling state QMFUS which was derived in [32]. Thus, this regime is identified as the ultrastrong coupling regime (US). Finally, for the parameter regime $8 \cdot 10^{-1} \leqslant \zeta < 7 \cdot 10^{1}$ the exact QMF shows variation with ζ that is not captured by neither weak nor ultrastrong coupling approximation. This is the intermediate coupling regime (IM), which is highly relevant from an experimental point of view, but there are no known analytical expressions that approximate the exact solution.

Beyond the zero temperature case, we compute $\langle s_x \rangle$ and $\langle s_z \rangle$ with the numerically exact QMF state over a wide range of coupling strengths and temperatures, and compare the results with those of the UW, WK, and US approximations allowing an error of $4 \cdot 10^{-3}$, as above. Figure 4(c) shows how pairs of ζ and T fall into various coupling regimes. One can see that, at elevated temperatures, the coupling regime boundaries shift towards higher coupling ζ. Thus at higher temperatures, $2k_B T/\hbar\omega_L \gtrsim 10$, the UW and WK approximations are valid at much higher coupling strengths ζ than at $T = 0$. At higher temperatures we also observe an emerging linear relation, $2k_B T/\hbar\omega_L \propto \zeta$, for all three regime boundaries. The temperature dependence of the

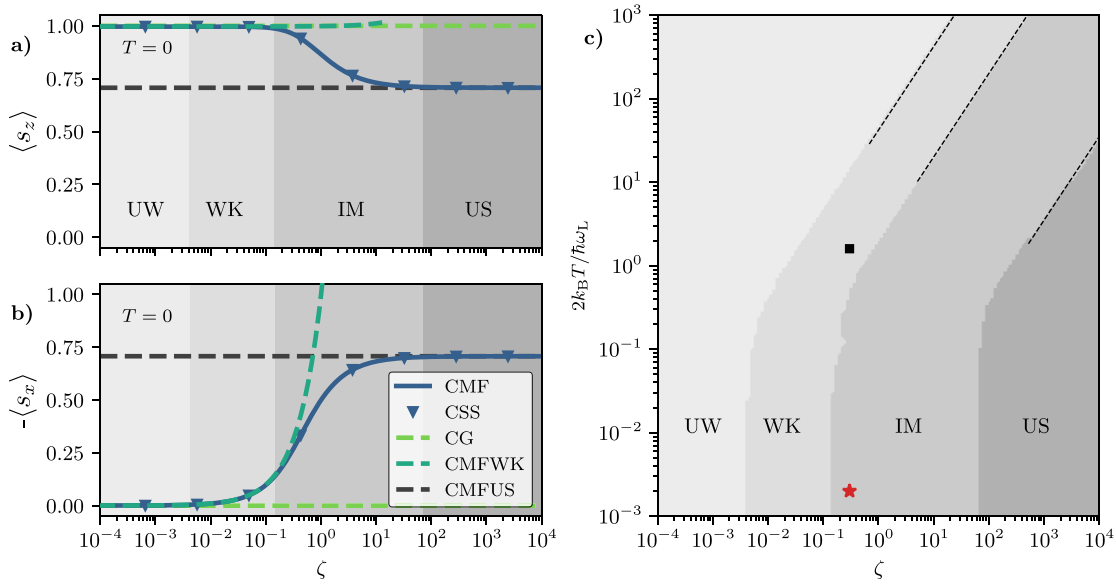

Figure 5. Classical coupling regimes at $T = 0$ and $T > 0$. Same plot as figure 4, but here for the equilibrium state of a *classical* spin vector **S** with Hamiltonian equation (3). A particular (T, ζ)-pair (red star) is identified for which the classical spin falls in the intermediate regime. For the same parameter pair, the *quantum* spin falls in the weak coupling regime, see red star in figure 4(c). Moving the classical red star upwards in temperature until it reaches a point (black square) in the weak coupling regime that is laterally distanced from the boundaries similar to the quantum star, figure 4(c), gives an effective temperature shift of $\Delta T = 1.6 \cdot 2\hbar\omega_L/k_B$. This example evidences significant differences between the environmental impact on quantum and classical equilibrium states.

border between the weak and intermediate coupling regime has previously been identified to be linear by Latune [70].

The quantum coupling regimes can now be compared to the corresponding regimes for a classical spin vector, shown in figures 5(a)–(c). Perhaps surprisingly, we find that the classical regime boundary values for ζ differ significantly from those for the quantum spin, e.g. by a factor of 10 for the WK approximation. This shift is exemplified by the red star, which indicates the same parameter pair (T, ζ) in both figures, figures 4(c) and 5(c). While the open quantum spin lies in the weak coupling regime, the classical one requires an intermediate coupling treatment. We suspect this quantum–classical distinctness comes from the fact that, while for a classical spin at zero temperature there is no noise induced by the bath, in the quantum case noise is present even at $T = 0$ K due to the bath's zero-point-fluctuations [43]. One may qualitatively interpret this additional noise as an effective temperature shift with respect to the classical case, by ca. $\Delta T = 1.6 \cdot 2\hbar\omega_L/k_B$, as indicated by the black square in figure 5(c).

To conclude, for any given coupling value ζ and temperature T, the two plots figures 4(c) and 5(c) provide a tool to judge whether a 'weak coupling' approximation is valid for the spin–boson model or not. We emphasise that, interestingly, the answer depends on whether one considers a quantum or a classical spin.

5. Conclusions

In this paper we have characterised the equilibrium properties of the θ–angled spin–boson model equations (1)–(4), in the quantum and classical regime. Firstly, for the classical case, we have derived a compact analytical expression for the equilibrium state of the spin, that is valid for arbitrary coupling to the harmonic reservoir. This is of great practical relevance as it allows one to analytically obtain all equilibrium properties of the spin at any coupling strength. It remains an open question [31] to find a similarly general analytical expressions for the quantum case.

Secondly, we have proven that the quantum MF partition function, including environmental terms, converges to its classical counterpart in the large-spin limit at all coupling strengths. This is the first time that such correspondence has been established for an *open* quantum system. Our results provide direct insight into the difference between quantum and classical states of a spin coupled to a noisy environment. Apart from being of purely fundamental interest, this will constitute key information for many quantum technologies [75], and ultimately links to the quantum supremacy debate.

Finally, we presented the first quantitative characterisation of the coupling parameter values that put the spin–boson model in the ultraweak, weak, intermediate, or ultrastrong coupling regime, both for the

quantum case as well as the classical setting. This classification will be important in many future studies of the spin–boson model, quantum or classical, for which it provides the tool to chose the correct approximation for a specific parameter set.

Data availability statements

The code used to produce figures 4 and 5 is publicly available online at https://github.com/quantum-exeter/SpinMFGS. It can be used to make analogous plots for a desired coupling angle θ and spin length S_0. The dynamical plots of figure 2 where done using the open-source library SpiDy.jl [57]. No new data were created or analysed in this study.

Acknowledgments

We thank Anton Trushechkin for stimulating discussions on the subject of this research. F C gratefully acknowledges funding from the Foundational Questions Institute Fund (FQXi-IAF19-01). S S is supported by a DTP grant from EPSRC (EP/R513210/1). SARH acknowledges funding from the Royal Society and TATA (RPG-2016-186). J A, F C, M B, and J C gratefully acknowledge funding from EPSRC (EP/R045577/1). J A thanks the Royal Society for support.

Note added

Since the original version of this paper was posted on the arXiv, a new approximate method to express the QMF in the IM regime has been proposed [76] based on the reaction coordinate mapping and polaron transformation. Furthermore, the impact of reservoir coupling to three spin components has been discussed for the quantum and classical case [77] and anisotropic spin-reservoir coupling effects have been identified [78]. Inclusion of the quantum reservoir in the prediction magnetisation curves [79] is showing high agreement with experimental curves of several materials, where classical models have not shown a match.

Appendix A. Tracing for spin and reservoir, in classical and quantum setting

A.1. Spin tracing in the classical setting

For a classical spin of length S_0, with components S_x, S_y, S_z, one can change into spherical coordinates, i.e.

$$\begin{aligned} &S_x = S_0 \sin\vartheta\cos\varphi, \quad S_y = S_0 \sin\vartheta \sin\varphi, \\ &S_z = S_0\cos\vartheta, \qquad \vartheta \in [0,\pi], \varphi \in [0,2\pi]. \end{aligned} \tag{A1}$$

Then, traces of functions $A(S_x, S_z)$ are evaluated as

$$\mathrm{tr}_{\mathrm{S}}^{\mathrm{cl}}\left[A\left(S_x,S_z\right)\right] = \frac{1}{4\pi}\int_0^{2\pi} \mathrm{d}\varphi \int_0^{\pi} \mathrm{d}\vartheta\, \sin\vartheta A\left(S_0\sin\vartheta\cos\varphi, S_0\cos\vartheta\right). \tag{A2}$$

A.2. Spin tracing in the quantum setting

For a quantum spin S_0, given any orthogonal basis $|m\rangle$, then the trace of functions of the spin operators $A(S_x, S_z)$ are evaluated as

$$\mathrm{tr}_{\mathrm{S}}^{\mathrm{qu}}\left[A\left(S_x,S_z\right)\right] = \sum_m \langle m|A\left(S_x,S_z\right)|m\rangle. \tag{A3}$$

A.3. Reservoir traces

When taking traces over the environmental degrees of freedom (in either the classical or quantum case), we ought to first discretise the energy spectrum of H_{R}. This is because, strictly speaking, the partition function for the reservoir, $Z_{\mathrm{R}} = \mathrm{tr}[\exp(-\beta H_{\mathrm{R}})]$, is not well defined in the continuum limit. Thus, we write

$$H_{\mathrm{R}} = \sum_{n=0}^{\infty} \frac{1}{2}\left(P_{\omega_n}^2 + \omega_n^2 X_{\omega_n}^2\right). \tag{A4}$$

Then, for example, the classical partition function of the environment is

$$Z_{\mathrm{R}}^{\mathrm{cl}} = \prod_{n=0}^{\infty}\left[\int_{-\infty}^{+\infty} \mathrm{d}X_{\omega_n} \int_{-\infty}^{\infty} \mathrm{d}P_{\omega_n} \mathrm{e}^{-\frac{\beta}{2}\left(P_{\omega_n}^2+\omega_n^2 X_{\omega_n}^2\right)}\right], \tag{A5}$$

and similarly for the quantum case.

Appendix B. Expectation values from the partition function

With the partition function of the MF we can proceed to calculate the S_z and S_x expectation values as follows.

B.1. Classical case

For the classical spin, from (7) we have the partition function

$$\tilde{Z}_{\mathrm{S}}^{\mathrm{cl}} = \frac{1}{4\pi}\int_0^{2\pi}\mathrm{d}\varphi \int_0^{\pi}\mathrm{d}\vartheta\, \sin\vartheta \mathrm{e}^{-\beta\left(-\omega_L S_z(\vartheta,\varphi)-QS_\theta^2(\vartheta,\varphi)\right)}. \tag{B1}$$

While obtaining the S_z expectation value is straightforward, the S_x case may seem less obvious. It is therefore convenient to do a change of coordinates

$$\begin{aligned} S_{z'}(\vartheta,\varphi) &= S_z(\vartheta,\varphi)\cos\theta - S_x(\vartheta,\varphi)\sin\theta, \\ S_{x'}(\vartheta,\varphi) &= S_x(\vartheta,\varphi)\cos\theta + S_z(\vartheta,\varphi)\sin\theta. \end{aligned} \tag{B2}$$

Defining $h_{x'} = -\omega_{\mathrm{L}}\sin\theta$, $h_{z'} = -\omega_{\mathrm{L}}\cos\theta$, we then have that

$$\tilde{Z}_{\mathrm{S}}^{\mathrm{cl}} = \frac{1}{4\pi}\int_0^{2\pi}\mathrm{d}\varphi \int_0^{\pi}\mathrm{d}\vartheta\, \sin\vartheta \mathrm{e}^{-\beta\left(h_{z'}S_{z'}(\vartheta,\phi)+h_{x'}S_{x'}(\vartheta,\phi)-QS_{z'}^2(\vartheta,\phi)\right)}, \tag{B3}$$

and we can obtain the $S_{z'}$ and $S_{x'}$ expectation values as usual, i.e.

$$\langle S_{x',z'}\rangle = -\frac{1}{\beta}\frac{\partial}{\partial h_{x',z'}}\log\tilde{Z}_{\mathrm{S}}^{\mathrm{cl}}. \tag{B4}$$

Finally, by linearity, we have that

$$\begin{aligned} \langle S_x\rangle &= \langle S_{x'}\rangle\cos\theta - \langle S_{z'}\rangle\sin\theta, \\ \langle S_z\rangle &= \langle S_{z'}\rangle\cos\theta + \langle S_{x'}\rangle\sin\theta. \end{aligned} \tag{B5}$$

B.2. Quantum case

For the quantum case we proceed in a completely analogous manner. We have that

$$\begin{aligned} \langle S_x\rangle &= \mathrm{tr}^{\mathrm{qu}}\left[S_x \mathrm{e}^{-\beta(-\omega_L S_z+S_\theta B+H_{\mathrm{R}})}\right], \\ \langle S_z\rangle &= \mathrm{tr}^{\mathrm{qu}}\left[S_z \mathrm{e}^{-\beta(-\omega_L S_z+S_\theta B+H_{\mathrm{R}})}\right]. \end{aligned} \tag{B6}$$

Starting from the partition function

$$Z_{\mathrm{SR}}^{\mathrm{qu}} = \mathrm{tr}^{\mathrm{qu}}\left[\mathrm{e}^{-\beta(-\omega_L S_z+S_\theta B+H_{\mathrm{R}})}\right], \tag{B7}$$

we define a new set of rotated operators,

$$\begin{aligned} S_{z'} &= S_z\cos\theta - S_x\sin\theta, \\ S_{x'} &= S_x\cos\theta + S_z\sin\theta, \end{aligned} \tag{B8}$$

and variables $h_{x'} = -\omega_{\mathrm{L}}\sin\theta$, $h_{z'} = -\omega_{\mathrm{L}}\cos\theta$, so that

$$Z_{\mathrm{SR}}^{\mathrm{qu}} = \mathrm{tr}^{\mathrm{qu}}\left[\mathrm{e}^{-\beta(h_{z'}S_{z'}+h_{x'}S_{x'}+S_{z'}B+H_{\mathrm{R}})}\right]. \tag{B9}$$

Then, we proceed in an analagous way as in (B4) and (B5).

B.3. Example: ultrastrong limit

Let us consider the quantum ultrastrong partition function,

$$\tilde{Z}^{\mathrm{qu}}_{\mathrm{S,US}} = \cosh\left(\beta\omega_L S_0 \cos\theta\right). \tag{B10}$$

Following the procedure outlined above, we have that $h_{z'} = -\omega_{\mathrm{L}}\cos\theta$, and therefore

$$\tilde{Z}^{\mathrm{qu}}_{\mathrm{S,US}} = \cosh\left(\beta S_0 h_{z'}\right). \tag{B11}$$

Therefore, the expectation values of the transformed observables are

$$\langle S_{x'}\rangle = -\frac{1}{\beta}\frac{\partial}{\partial h_{x'}}\log\ \tilde{Z}^{\mathrm{qu}}_{\mathrm{S,US}} = 0, \tag{B12}$$

$$\begin{aligned}\langle S_{z'}\rangle &= -\frac{1}{\beta}\frac{\partial}{\partial h_{z'}}\log\ \tilde{Z}^{\mathrm{qu}}_{\mathrm{S,US}} = -S_0\tanh\left(\beta S_0 h_{z'}\right)\\ &= -S_0\tanh\left(\beta\omega_L S_0\cos\theta\right).\end{aligned} \tag{B13}$$

Therefore, in the original variables we have

$$\langle S_x\rangle = S_0\sin\theta\tanh\left(\beta\omega_L S_0\cos\theta\right), \tag{B14}$$

$$\langle S_z\rangle = -S_0\cos\theta\tanh\left(\beta\omega_L S_0\cos\theta\right), \tag{B15}$$

in agreement with what is later obtained in appendix G directly from the MF in the ultra-strong limit.

Appendix C. Derivation of classical MF state for arbitrary coupling

In this section we derive the mean force Gibbs state of the classical spin for arbitrary coupling strength. As discussed in appendix A, we discretise the environmental degrees of freedom, and thus we have for the total Hamiltonian, (3)

$$H_{\mathrm{tot}} = -\omega_L S_z + \sum_{n=0}^{\infty}\left[\frac{1}{2}\left(P^2_{\omega_n} + \omega_n^2 X^2_{\omega_n}\right) + S_\theta C_{\omega_n} X_{\omega_n}\right]. \tag{C1}$$

On 'completing the square', we get

$$H_{\mathrm{tot}} = -\omega_L S_z + \sum_{n=0}^{\infty}\frac{1}{2}\left[P^2_{\omega_n} + \omega_n^2\left(X_{\omega_n} - \frac{S_\theta C_{\omega_n}}{\omega_n^2}\right)^2 - \frac{\left(S_\theta C_{\omega_n}\right)^2}{2\omega_n^2}\right]. \tag{C2}$$

The partition function is then,

$$Z^{\mathrm{cl}}_{\mathrm{SR}} = \frac{1}{4\pi}\int_0^{2\pi}\mathrm{d}\varphi\int_0^{\pi}\mathrm{d}\vartheta\,\sin\vartheta\mathrm{e}^{-\beta H_{\mathrm{eff}}}Z^{\mathrm{cl}}_{\mathrm{R}}. \tag{C3}$$

Here, there appears an effective system Hamiltonian given by

$$H_{\mathrm{eff}} \equiv -\omega_L S_z - Q S_\theta^2 \tag{C4}$$

where the reorganization energy Q, is given by equation (5) of the main text, and

$$Z^{\mathrm{cl}}_{\mathrm{R}} = \prod_n\int_{-\infty}^{\infty}\mathrm{d}X_{\omega_n}\int_{-\infty}^{\infty}\mathrm{d}P_{\omega_n}\mathrm{e}^{-\frac{1}{2}\beta\left(P^2_{\omega_n}+\omega_n^2\left(X_{\omega_n}-\frac{S_\theta C_{\omega_n}}{\omega_n^2}\right)^2\right)}, \tag{C5}$$

is the partition function for the reservoir only. Note that, despite seemingly depending on the spin coordinates, this last integral coincides with the reservoir partition function since once one carries out the Gaussian integral, the dependence on S_θ vanishes.

While it is possible to derive an expression for Z_{R}, its details are not needed as it depends solely on reservoir variables and can be divided out to yield the system's MF partition function,

$$\tilde{Z}^{\mathrm{cl}}_{\mathrm{S}} = \frac{Z^{\mathrm{cl}}_{\mathrm{SR}}}{Z^{\mathrm{cl}}_{\mathrm{R}}} = \frac{1}{4\pi}\int_0^{2\pi}\mathrm{d}\varphi\int_0^{\pi}\mathrm{d}\vartheta\,\sin\vartheta\mathrm{e}^{-\beta H_{\mathrm{eff}}}, \tag{C6}$$

where $H_{\rm eff}$ includes all spin terms independent of the coordinates of the environment. Finally, the MF is given by

$$\tau_{\rm MF} = \frac{1}{\tilde{Z}_{\rm S}^{\rm cl}} {\rm e}^{-\beta H_{\rm eff}}, \tag{C7}$$

which is precisely equation (7) of the main text.

In terms of polar coordinates, we have $S_\theta = S_0\left(\cos\vartheta\cos\theta - \sin\vartheta\cos\varphi\sin\theta\right)$, and then

$$H_{\rm eff}(\vartheta,\varphi) = -\omega_L S_0\cos\vartheta - S_0^2 Q\left(\cos\theta\cos\vartheta - \sin\theta\sin\vartheta\cos\varphi\right)^2. \tag{C8}$$

The equilibrium state of the spin is then entirely determined by $\tilde{Z}_{\rm S}^{\rm cl}$. The classical expectation values for the spin components S_z and S_x are then given by

$$\langle s_z\rangle = \frac{\langle S_z\rangle}{S_0} = \frac{1}{\tilde{Z}_{\rm S}^{\rm cl}}\int_0^{2\pi}{\rm d}\varphi\int_0^{\pi}{\rm d}\vartheta\,\sin\vartheta\cos\vartheta{\rm e}^{-\beta H_{\rm eff}(\vartheta,\varphi)} \tag{C9}$$

$$\langle s_x\rangle = \frac{\langle S_x\rangle}{S_0} = \frac{1}{\tilde{Z}_{\rm S}^{\rm cl}}\int_0^{2\pi}{\rm d}\varphi\cos\varphi\int_0^{\pi}{\rm d}\vartheta\,\sin^2\vartheta{\rm e}^{-\beta H_{\rm eff}(\vartheta,\varphi)}. \tag{C10}$$

The integral expressions for the expectation values above cannot in general be expressed in a closed form, but can be readily evaluated numerically for arbitrary coupling strength Q.

Appendix D. Quantum–classical correspondence for the MF partition functions

Starting from equation (F27) of the main text, we now 'complete the square' for the combination

$$h_{\rm R} + s_\theta\int_0^\infty {\rm d}\omega C_\omega\sqrt{S_0}x_\omega, \tag{D1}$$

to arrive at

$$\frac{1}{2}\int_0^\infty{\rm d}\omega\left(p_\omega^2 + \omega^2\left(x_\omega + s_\theta\frac{C_\omega\sqrt{S_0}}{\omega^2}\right)^2\right) - s_\theta^2 S_0 Q(S_0) = h_{\rm R}^{\rm shift} - s_\theta^2 S_0 Q(S_0), \tag{D2}$$

where $Q(S_0) = \int_0^\infty {\rm d}\omega C_\omega^2(S_0)/(2\omega^2)$ is the reorganisation energy, see (5). Note that because of the scaling $C_\omega \propto 1/\sqrt{S_0}$, the product $S_0 Q(S_0) = \alpha\omega_{\rm L}$ is independent of S_0. Here, we have defined the reservoir Hamiltonian

$$h_{\rm R}^{\rm shift} = \frac{1}{2}\int_0^\infty{\rm d}\omega\left(p_\omega^2 + \omega^2\left(x_\omega + s_\theta\frac{C_\omega\sqrt{S_0}}{\omega^2}\right)^2\right), \tag{D3}$$

where the oscillator centres have been shifted.

Applying (8) to the total spin-reservoir Hamiltonian $H_{\rm tot}$, and immediately taking the reservoir trace on both sides, gives

$$\begin{aligned}\lim_{S_0\to\infty}\frac{\hbar}{2S_0+\hbar}Z_{\rm SR}^{\rm qu}(\beta,S_0,\alpha) &= \lim_{S_0\to\infty}\frac{\hbar}{2S_0+\hbar}{\rm tr}_{\rm SR}^{\rm qu}\left[{\rm e}^{-\beta'\left(-\omega_L S_z + h_{\rm R}^{\rm shift} - s_\theta^2\,\alpha\,\omega_{\rm L}\right)}\right]\\ &= \lim_{S_0\to\infty}\frac{1}{4\pi}\int_0^{2\pi}{\rm d}\varphi\int_0^{\pi}{\rm d}\vartheta\,\sin\vartheta{\rm tr}_{\rm R}^{\rm qu}\left[{\rm e}^{-\beta'\left(-\omega_{\rm L}\cos\vartheta + h_{\rm R}^{\rm shift} - s_\theta^2(\vartheta,\phi')\,\alpha\,\omega_{\rm L}\right)}\right]\\ &= \lim_{S_0\to\infty}\frac{1}{4\pi}\int_0^{2\pi}{\rm d}\varphi\int_0^{\pi}{\rm d}\vartheta\,\sin\vartheta{\rm e}^{-\beta'\left(-\omega_{\rm L}\cos\vartheta - s_\theta^2(\vartheta,\phi')\,\alpha\,\omega_{\rm L}\right)}{\rm tr}_{\rm R}^{\rm qu}\left[{\rm e}^{-\beta' h_{\rm R}^{\rm shift}}\right],\end{aligned} \tag{D4}$$

where the trace over the reservoir now factors out and

$$s_\theta(\vartheta,\phi') = \cos\theta\cos\vartheta - \sin\theta\cos\varphi\sin\vartheta. \tag{D5}$$

The reservoir trace factor gives

$$\begin{aligned}{\rm tr}_{\rm R}^{\rm qu}\left[{\rm e}^{-\beta' h_{\rm R}^{\rm shift}}\right] &= {\rm tr}_{\rm R}^{\rm qu}\left[{\rm e}^{-\beta\frac{1}{2}\int_0^\infty{\rm d}\omega\left(P_\omega^2+\omega^2(X_\omega+\mu_\omega)^2\right)}\right]\\ &= Z_{\rm R}^{\rm qu}(\beta),\end{aligned} \tag{D6}$$

with $\mu_\omega = S_\theta \frac{C_\omega}{\omega^2}$ a shift in the centre position of the oscillators. The operators $X_\omega + \mu_\omega$ have the same commutation relations with the P_ω as the X_ω themselves. Thus such a shift does not affect the trace and the result is the bare quantum reservoir partition function at inverse temperature β, i.e. $Z_{\rm R}^{\rm qu}(\beta)$.

Dividing by $Z_{\rm R}^{\rm qu}(\beta)$ on both sides, putting it all together, we find

$$\lim_{S_0\to\infty} \frac{\hbar}{2S_0+\hbar} \frac{Z_{\rm SR}^{\rm qu}(\beta, S_0, \alpha)}{Z_{\rm R}^{\rm qu}(\beta)} = \frac{1}{4\pi}\int_0^{2\pi} {\rm d}\varphi \int_0^{\pi} {\rm d}\vartheta \sin\vartheta\, {\rm e}^{-\beta'\left(-\omega_{\rm L}\cos\vartheta - s_\theta^2(\vartheta,\phi')\,\alpha\,\omega_{\rm L}\right)}, \tag{D7}$$

where we have dropped the limit symbol since there is no dependence on S_0.

Now we may replace again $\beta' = \beta S_0$, and the RHS emerges as the spin's classical mean force partition function $\tilde{Z}_{\rm S}^{\rm cl}(\beta S_0, \alpha)$, cf (7), where the classical trace is taken according to (A2). Moreover, the fraction of total quantum partition function divided by bare reservoir partition function is the quantum mean force partition function [67, 68]. Thus, we conclude:

$$\lim_{S_0\to\infty} \frac{\hbar}{2S_0+\hbar} \tilde{Z}_{\rm S}^{\rm qu}(\beta, S_0, \alpha) = \lim_{S_0\to\infty} \frac{\hbar}{2S_0+\hbar} \frac{Z_{\rm SR}^{\rm qu}(\beta, S_0, \alpha)}{Z_{\rm R}^{\rm qu}(\beta)} = \tilde{Z}_{\rm S}^{\rm cl}(\beta S_0, \alpha). \tag{D8}$$

Appendix E. Quantum reaction coordinate mapping

The Reaction Coordinate mapping method [71–74] is a technique for dealing with systems strongly coupled to bosonic environments. To do so, it isolates a single collective environmental degree of freedom, the so called 'reaction coordinate' (RC), that interacts with the system via an effective Hamiltonian. The rest of the environmental degrees of freedom manifest as a new bosonic environment coupled to the RC. Concretely, for our total Hamiltonian (3), the effective Hamiltonian that we have to consider is

$$H_{\rm tot}^{\rm RC} = H_{\rm S} + H_{\rm RC} + H_{\rm int}^{\rm RC} + H_{\rm int}^{\rm res} + H_{\rm res}, \tag{E1}$$

where $H_{\rm RC}$ is the Hamiltonian of the RC mode,

$$H_{\rm RC} = \hbar\Omega_{\rm RC} a^\dagger a, \tag{E2}$$

with $a^\dagger$ the creation operator of a quantum harmonic oscillator of frequency $\Omega_{\rm RC}$; $H_{\rm int}^{\rm RC}$ is the spin–RC interaction

$$H_{\rm int}^{\rm RC} = \lambda_{\rm RC} S_\theta \left(a + a^\dagger\right), \tag{E3}$$

where $\lambda_{\rm RC}$ determines the the coupling strength between the RC mode and the spin; $H_{\rm res} = \int {\rm d}\omega (p_\omega^2 + \omega^2 q_\omega^2)/2$ is the Hamiltonian of the residual bosonic bath; and finally the residual bath-RC interaction $H_{\rm int}^{\rm res}$ is

$$H_{\rm int}^{\rm res} = \left(a + a^\dagger\right) \int_0^\infty {\rm d}\omega \sqrt{2\omega J_{\rm RC}} q_\omega, \tag{E4}$$

with $J_{\rm RC}$ the spectral density of the residual bath.

Given $H_{\rm tot}$, for an appropriate choice of $J_{\rm RC}$ (which depends on the original Hamiltonian spectral density and coupling), it has been proven that the reduced dynamics of the spin under $H_{\rm tot}$ are exactly the same as those of the spin under the effective Hamiltonian $H_{\rm tot}^{\rm RC}$ [73]. In general, the mapping between the original spectral density, J_ω, and that of the RC Hamiltonian, $J_{\rm RC}$, is hard to find. However, one particular case were there is a simple closed form for $J_{\rm RC}$ is that of a Lorentzian spectral density J_ω (see main text). In such case, the $J_{\rm RC}$ spectral density is exactly Ohmic [71–73], i.e. has the form

$$J_{\rm RC} = \gamma_{\rm RC}\omega {\rm e}^{-\omega/\omega_{\rm c}}, \qquad \omega_{\rm c} \to \infty. \tag{E5}$$

Furthermore, the RC effective Hamiltonian parameters ($\Omega_{\rm RC}$, $\lambda_{\rm RC}$ and $\gamma_{\rm RC}$) are given in terms of the Lorentzian parameters by

$$\Omega_{\rm RC} = \omega_0, \tag{E6}$$

$$\lambda_{\rm RC} = \sqrt{Q\omega_0}, \tag{E7}$$

$$\gamma_{\rm RC} = \frac{\Gamma}{2\pi\omega_0}. \tag{E8}$$

Noticeably, by appropriately choosing Q, Γ, and ω_0, we can have an initial Hamiltonian with arbitrarily strong coupling to the full environment (i.e. arbitrarily strong Q), while having arbitrarily small coupling to the residual bath of the RC Hamiltonian (i.e. arbitrarily small $\gamma_{\rm RC}$).

As mentioned, it has been shown that the reduced spin dynamics under $H_{\rm tot}$ with Lorentzian spectral density (see main text) is exactly the same as the reduced spin dynamics under $H_{\rm tot}^{\rm RC}$ with spectral density (E5). In particular, the steady state of the spin will also be the same. Therefore, it is reasonable to expect that the spin MF state obtained with $H_{\rm tot}$ will be the same as the spin MF state for $H_{\rm tot}^{\rm RC}$, i.e.

$$\tau_{\rm MF} = \tilde{Z}_{\rm S}^{-1}{\rm tr}_{\rm R}\left[{\rm e}^{-\beta H_{\rm tot}}\right] = \tilde{Z}_{\rm S}'^{-1}{\rm tr}_{\rm R}\left[{\rm e}^{-\beta H_{\rm tot}^{\rm RC}}\right]. \tag{E9}$$

We now assume that $\gamma_{\rm RC}$ is arbitrarily small, so that the MF state is simply going to be given by the Gibbs state of spin+RC, i.e.

$$\tau_{\rm MF} = \tilde{Z}_{\rm S}'^{-1}{\rm tr}_{\rm R}\left[{\rm e}^{-\beta H_{\rm tot}^{\rm RC}}\right] \approx \tilde{Z}_{\rm S}''^{-1}{\rm tr}_{\rm R}\left[{\rm e}^{-\beta\left(H_{\rm S}+\Omega_{\rm RC}a^\dagger a+\lambda_{\rm RC}S_\theta\left(a+a^\dagger\right)\right)}\right]. \tag{E10}$$

It is key here to observe that the condition $\gamma_{\rm RC}\to 0$ does not imply any constraint on the coupling strength to the original environment, since we can always choose Γ and ω_0 so that $\gamma_{\rm RC}$ is arbitrarily small, while allowing Q to be arbitrarily large.

Finally, to numerically obtain the MF state, since unfortunately (E10) does not have a general closed form, we numerically evaluate (E10) by diagonalising the full Hamiltonian and then taking the partial trace over the RC. To numerically diagonalise this Hamiltonian we have to choose a cutoff on the number of energy levels of the RC harmonic oscillator. This cutoff was chosen by increasing the number of levels until observing convergence of the numerical results.

Appendix F. Quantum to classical limit in the weak coupling approximation

In this section we explicitly compute the large spin limit for the weak coupling expressions of the classical and quantum mean force Gibbs states. These results are used in the characterisation of the different coupling regimes.

Since we are going to perform perturbative expansions in the coupling strength, in what follows we introduce, for book-keeping purposes, an adimensional parameter λ in the interaction, so that $H_{\rm int}$ now reads

$$H_{\rm int} = \lambda S_\theta\int_0^\infty {\rm d}\omega C_\omega X_\omega. \tag{F1}$$

This will allow us to properly keep track of the order of each term in the expansion. Finally, at the end of the calculations we will take $\lambda = 1$.

F.1. Classical spin: weak coupling

Here, we derive the classical weak coupling expectation values starting from the exact MF found in appendix C. The effective Hamiltonian, with the inclusion of the parameter λ now reads

$$H_{\rm eff} = -\omega_L S_z - \lambda^2 Q S_\theta^2. \tag{F2}$$

For weak coupling, the expressions for $\tilde{Z}_{\rm S}^{\rm cl}$, $\langle S_z\rangle$ and $\langle S_x\rangle$ can be approximated by treating the term $\lambda^2 S_0^2 Q$ as a perturbation. Therefore, expanding $\exp[-\beta H_{\rm eff}]$ to lowest order in λ we have

$${\rm e}^{-\beta H_{\rm eff}} = {\rm e}^{\beta\omega_L S_0\cos\vartheta}\left[1+\beta\lambda^2 S_0^2 Q\left(\cos\theta\cos\vartheta-\sin\theta\sin\vartheta\cos\varphi\right)^2\right]+\mathcal{O}\left(\lambda^4\right), \tag{F3}$$

from which we can determine the weak coupling limit of the classical spin partition function and spin expectation values.

F.1.1. Standard Gibbs results for a classical spin

First, here we write the partition function and spin expectation values for a classical spin in the standard Gibbs state for the bare Hamiltonian $H_{\rm S}$ (i.e. in the limit of vanishing coupling, $\lambda = 0$). These expressions will be useful to later on to write the second order corrections.

For the partition function we have that

$$Z_0^{\rm cl} = \frac{1}{4\pi}\int_0^{2\pi} {\rm d}\varphi \int_0^{\pi} {\rm d}\vartheta\, \sin\vartheta \exp\left[\beta\omega_L S_0 \cos\vartheta\right] = \frac{\sinh\left(\beta\omega_L S_0\right)}{\beta\omega_L S_0}. \tag{F4}$$

The expectation value of S_x is trivially 0 by symmetry, i.e.

$$\langle S_x\rangle_0 = \frac{1}{Z_0^{\rm cl}} S_0 \int_0^{2\pi} {\rm d}\varphi \cos\varphi \int_0^{\pi} {\rm d}\vartheta\, \sin^2\vartheta {\rm e}^{\beta\omega_L S_0\cos\vartheta} = 0. \tag{F5}$$

For the expectation value of the powers of S_z (which will be useful later), we have

$$\langle S_z^n\rangle_0 = \frac{2\pi}{Z_0^{\rm cl}} S_0^n \int_0^{\pi} {\rm d}\vartheta\, \sin\vartheta\cos^n\vartheta\, {\rm e}^{\beta\omega_L S_0\cos\vartheta}. \tag{F6}$$

In particular, we find

$$\langle S_z\rangle_0 = S_0\coth\left(\beta\omega_L S_0\right) - \frac{1}{\beta\omega_{\rm L}}, \tag{F7}$$

$$\langle S_z^2\rangle_0 = S_0^2 - \frac{2S_0\coth\left(\beta\omega_L S_0\right)}{\beta\omega_{\rm L}} + \frac{2}{\left(\beta\omega_{\rm L}\right)^2}, \tag{F8}$$

$$\langle S_z^3\rangle_0 = S_0^3\coth\left(\beta\omega_L S_0\right) - \frac{3S_0^2}{\beta\omega_{\rm L}} + \frac{6S_0\coth\left(\beta\omega_L S_0\right)}{\left(\beta\omega_{\rm L}\right)^2} - \frac{6}{\left(\beta\omega_{\rm L}\right)^3}. \tag{F9}$$

F.1.2. Classical spin partition function for weak coupling

Expanding the partition function to second order in λ we find that

$$\tilde{Z}_{\rm S}^{\rm cl} = \frac{1}{4\pi}\int_0^{2\pi}{\rm d}\varphi\int_0^{\pi}{\rm d}\vartheta\,\sin\vartheta\left[{\rm e}^{\beta\omega_L S_0\cos\vartheta} + \frac{\beta\lambda^2 S_0^2 Q}{4\pi}{\rm e}^{\beta\omega_L S_0\cos\vartheta}\left(\cos\theta\cos\vartheta - \sin\theta\sin\vartheta\cos\varphi\right)^2\right] + \mathcal{O}(\lambda^4). \tag{F10}$$

The first term can be recognised as the partition function for the bare system, $Z_0^{\rm cl}$. The φ' integral in the second term is straightforward to perform,

$$\tilde{Z}_{\rm S}^{\rm cl} = Z_0^{\rm cl} + \frac{1}{2}\beta\lambda^2 S_0^2 Q\int_0^{\pi}{\rm d}\vartheta\,\sin\vartheta{\rm e}^{\beta\omega_L S_0\cos\vartheta}\left[\left(3\cos^2\theta - 1\right)\cos^2\vartheta + \sin^2\theta\right] + \mathcal{O}(\lambda^4). \tag{F11}$$

We typically require the inverse of the partition function, which to lowest order in the perturbation is

$$\tilde{Z}_{\rm S}^{\rm cl} = \left(Z_0^{\rm cl}\right)^{-1}\left[1 - \pi\beta\lambda^2 S_0^2 Q Z_0^{-1}\int_0^{\pi}{\rm d}\vartheta\,\sin\vartheta{\rm e}^{\beta\omega_L S_0\cos\vartheta}\left(\left(3\cos^2\theta - 1\right)\cos^2\vartheta + \sin^2\theta\right)\right] + \mathcal{O}(\lambda^4). \tag{F12}$$

Now turning to the expectation value $\langle S_z\rangle$, given in equation (C9), and carrying out the same lowest order expansion we get

$$\langle S_z\rangle = \langle S_z\rangle_0 + \frac{1}{2}\beta\lambda^2 Q\left[\left(3\cos^2\theta - 1\right)\left(\langle S_z^3\rangle_0 - \langle S_z\rangle_0\langle S_z^2\rangle_0\right)\right] + \mathcal{O}\left(\lambda^4\right). \tag{F13}$$

This result will be compared later to the quantum weak coupling result obtained in the large spin (classical) limit.

F.1.3. Classical $\langle S_x\rangle$ for weak coupling

A similar calculation can be followed for $\langle S_x\rangle$, the main difference being in the handling of the φ' integral. Thus, we find

$$\langle S_x\rangle = -\tfrac{1}{2}\sin 2\theta\beta\lambda^2 Q\left(\langle S_z\rangle_0 S_0^2 - \langle S_z^3\rangle_0\right) + \mathcal{O}\left(\lambda^4\right), \tag{F14}$$

where we have used that $Z_0/\tilde{Z}_{\rm S}^{\rm cl} = 1$ to lowest order.

Using the zeroth order expressions for $\langle S_z\rangle_0$ and $\langle S_z^3\rangle_0$ from (F7) we get the result in terms of the scaled temperature $\beta' = \beta S_0$

$$\langle S_x\rangle = -\frac{\sin 2\theta\lambda^2 S_0 Q}{\omega_{\rm L}}\left(1 - \frac{3\coth(\beta'\omega_{\rm L})}{\beta'\omega_{\rm L}} + \frac{3}{(\beta'\omega_{\rm L})^2}\right) + \mathcal{O}(\lambda^4). \tag{F15}$$

This result will be compared later to the quantum weak coupling result obtained in the large spin (classical) limit.

F.2. Quantum spin: weak coupling

In general, the quantum mean force Gibbs state is given by

$$\tau_{\mathrm{MF}} = \frac{\mathrm{tr}_{\mathrm{R}}^{\mathrm{qu}}\left[\mathrm{e}^{-\beta H_{\mathrm{tot}}}\right]}{Z_{\mathrm{tot}}^{\mathrm{qu}}}, \tag{F16}$$

with H_{tot} given by equation (3) of the main text. Unfortunately, determining the form of τ_{MF} and the various expectation values for the spin components is unfeasible in the general case, but limiting forms are available. Here we derive the spin expectation values in the weak coupling limit, and then later on take the large spin limit to explicitly verify the quantum-to-classical transition.

F.2.1. Standard Gibbs results for a quantum spin

Here, we present the results of the standard Gibbs state for the quantum spin (i.e. in the limit of vanishing coupling, $\lambda = 0$). The Gibbs state for the system's bare Hamiltonian is

$$\tau_{\mathrm{S}} = \frac{\mathrm{e}^{\beta\omega_L S_z}}{Z_{\mathrm{S}}^{\mathrm{qu}}}, \quad Z_{\mathrm{S}}^{\mathrm{qu}} = \mathrm{tr}\left[\mathrm{e}^{\beta\omega_L S_z}\right]. \tag{F17}$$

We also have that $[\tau_{\mathrm{S}}, S_z] = 0$. The trace is readily evaluated, yielding the partition function

$$Z_0^{\mathrm{qu}} = \frac{\sinh\beta\omega_{\mathrm{L}}\left(S_0 + \frac{\hbar}{2}\right)}{\sinh\frac{\hbar}{2}\beta\omega_{\mathrm{L}}}, \tag{F18}$$

from which we can derive the expectation values of S_z, S_z^2 and S_z^3,

$$\langle S_z^n\rangle_0 = \frac{1}{Z_0^{\mathrm{qu}}}\frac{\mathrm{d}^n}{\mathrm{d}\left(\beta\omega_{\mathrm{L}}\right)^n} Z_0^{\mathrm{qu}}. \tag{F19}$$

We find,

$$\langle S_z\rangle_0 = \left(S_0 + \tfrac{\hbar}{2}\right)\coth\left(\beta\omega_{\mathrm{L}}\left(S_0 + \tfrac{\hbar}{2}\right)\right) - \tfrac{\hbar}{2}\coth\left(\tfrac{\hbar}{2}\beta\omega_{\mathrm{L}}\right) \tag{F20}$$

$$\langle S_z^2\rangle_0 = \left(S_0 + \tfrac{\hbar}{2}\right)^2 - \hbar\left(S_0 + \tfrac{\hbar}{2}\right)\coth\left(\tfrac{\hbar}{2}\beta\omega_{\mathrm{L}}\right)\coth\left(\beta\omega_{\mathrm{L}}\left(S_0 + \tfrac{\hbar}{2}\right)\right) + \tfrac{\hbar^2}{4}\left(2\coth^2\left(\tfrac{\hbar}{2}\beta\omega_{\mathrm{L}}\right) - 1\right) \tag{F21}$$

$$\begin{aligned}\langle S_z^3\rangle_0 = {} & \left(S_0 + \tfrac{\hbar}{2}\right)^3\coth\left(\beta\omega_{\mathrm{L}}\left(S_0 + \tfrac{\hbar}{2}\right)\right) - \tfrac{3\hbar}{2}\left(S_0 + \tfrac{\hbar}{2}\right)^2\coth\left(\tfrac{\hbar}{2}\beta\omega_{\mathrm{L}}\right) \\ & + \tfrac{3\hbar^2}{4}\left(S_0 + \tfrac{\hbar}{2}\right)\coth\left(\beta\omega_{\mathrm{L}}\left(S_0 + \tfrac{\hbar}{2}\right)\right)\left(2\coth^2\left(\tfrac{\hbar}{2}\beta\omega_{\mathrm{L}}\right) - 1\right) \\ & - \tfrac{3\hbar^3}{4}\coth^3\left(\tfrac{\hbar}{2}\beta\omega_{\mathrm{L}}\right) + \tfrac{5\hbar^3}{8}\coth\left(\tfrac{\hbar}{2}\beta\omega_{\mathrm{L}}\right).\end{aligned} \tag{F22}$$

F.2.2. General form of weak coupling density operator

For a total Hamiltonian $H_{\mathrm{S}} + H_{\mathrm{R}} + H_{\mathrm{int}}$ with interaction of the form $H_{\mathrm{int}} = \lambda XB$, the general expression for the *unnormalised* mean force state to second order in the interaction is given by [32]

$$\begin{aligned}\tilde{\rho}^{(2)} = {} & \tau_{\mathrm{S}} + \lambda^2\sum_n\left(\left[X_n^\dagger, \tau_{\mathrm{S}}X_n\right]A'_\beta(\omega_n) + \beta\tau_{\mathrm{S}}X_nX_n^\dagger A_\beta(\omega_n)\right) \\ & + \lambda^2\sum_{m\neq n}\omega_{mn}^{-1}\left(\left[X_m, X_n^\dagger\tau_{\mathrm{S}}\right] + \left[\tau_{\mathrm{S}}X_n, X_m^\dagger\right]\right)A_\beta(\omega_n),\end{aligned} \tag{F23}$$

where the system operator X is expanded in terms of the energy eigenoperators X_n

$$X = \sum_n X_n, \tag{F24}$$

with $[H_{\mathrm{S}}, X_n] = \omega_n X_n$, and ω_n are Bohr frequencies for the system. We have $X_n^\dagger = X_{-n}$ and $\omega_n = -\omega_{-n}$. The quantities $A_\beta(\omega_n)$ are determined by the correlation properties of the reservoir operator B and are given by

$$A_\beta(\omega_n) = \int_0^\infty \mathrm{d}\omega J_\omega\left(\frac{n_\beta(\omega)+1}{\omega-\omega_n} - \frac{n_\beta(\omega)}{\omega+\omega_n}\right), \tag{F25}$$

$$A'_\beta(\omega_n) = \int_0^\infty \mathrm{d}\omega\frac{J_\omega}{\hbar}\left(\frac{n_\beta(\omega)+1}{(\omega-\omega_n)^2} + \frac{n_\beta(\omega)}{(\omega+\omega_n)^2}\right). \tag{F26}$$

We can separate out the particular case of $\omega_n = 0$, for which we find

$$A_\beta(0) = \int_0^\infty \mathrm{d}\omega \, \frac{J_\omega}{\omega} = Q. \tag{F27}$$

It turns out that we will require various symmetric and antisymmetric combinations of $A_\beta(\omega_n)$ and $A'_\beta(\omega_n)$. [Note that in the following (and in the initial definition of the quantity $A'_\beta(\omega_n)$), the dash indicates a derivative wrt to the argument ω_n. Thus the quantity $A'_\beta(-\omega_n)$ is a derivative wrt $-\omega_n$, i.e. $A'_\beta(-\omega_n) = -\mathrm{d}A_\beta(-\omega_n)/\mathrm{d}\omega_n$, whereas, as usual, $A'_\beta(\omega_n) = \mathrm{d}A_\beta(\omega_n)/\mathrm{d}\omega_n$ etc.] Therefore, we define

$$\Sigma(\omega_n) = A_\beta(\omega_n) + A_\beta(-\omega_n) = 2\int_0^\infty \mathrm{d}\omega J_\omega \frac{\omega}{\omega^2 - \omega_n^2} \tag{F28}$$

$$\Delta_\beta(\omega_n) = A_\beta(\omega_n) - A_\beta(-\omega_n) = 2\omega_n \int_0^\infty \mathrm{d}\omega J_\omega \frac{1}{\omega^2 - \omega_n^2} \coth\left(\tfrac{1}{2}\beta\hbar\omega\right) \tag{F29}$$

$$\Delta'_\beta(\omega_n) = A'_\beta(\omega_n) + A'_\beta(-\omega_n) = 2\int_0^\infty \mathrm{d}\omega \frac{J_\omega}{\hbar} \frac{\left(\omega^2 + \omega_n^2\right)}{\left(\omega^2 - \omega_n^2\right)^2} \coth\left(\tfrac{1}{2}\beta\hbar\omega\right) \tag{F30}$$

$$\Sigma'(\omega_n) = A'_\beta(\omega_n) - A'_\beta(-\omega_n) = 4\omega_n \int_0^\infty \mathrm{d}\omega \frac{J_\omega}{\hbar} \frac{\omega}{\left(\omega^2 - \omega_n^2\right)^2}. \tag{F31}$$

F.2.3. Normalising the second order MF state

From (F23) we get the second order partition function

$$\tilde{Z}_\mathrm{S}^{(2)} = \mathrm{tr}\left[\tilde{\rho}^{(2)}\right] = 1 + \beta\lambda^2 \sum_n \mathrm{tr}\left[\tau_\mathrm{S} X_n X_n^\dagger\right] A_\beta(\omega_n). \tag{F32}$$

This can be used directly to evaluate the second order expectation value $\langle S_z\rangle^{(2)}$, but instead we will proceed to derive the second order MF state. This normalised state can be arrived at as in [32], where a binomial approximation in used. Those expressions however seem to imply that the validity of the approximation depends on the temperature, with the approximation breaking down at low enough temperatures. Here we proceed in an alternative way that shows that there is no such limitation.

The exact density operator is

$$\tau_\mathrm{MF}(\lambda) = \frac{\tilde{\rho}(\lambda)}{\tilde{Z}_\mathrm{S}^\mathrm{qu}(\lambda)}, \tag{F33}$$

where the dependence on λ is made explicit, and write

$$\tau_\mathrm{MF}(\lambda) = \tau_\mathrm{MF}(0) + \tfrac{1}{2}\lambda^2 \frac{\mathrm{d}^2\tau_\mathrm{MF}}{\mathrm{d}\lambda^2}(0) + \mathcal{O}\left(\lambda^4\right), \tag{F34}$$

where $\tau_\mathrm{MF}(0) = \tau_\mathrm{S}$ is the Gibbs state of the system in the limit of vanishingly small system-reservoir coupling, and it has been recognised that odd order contributions will vanish.

From this we also find

$$\tilde{Z}_\mathrm{S}^\mathrm{qu}(\lambda) = 1 + \tfrac{1}{2}\lambda^2 \frac{\mathrm{d}^2\tilde{Z}_\mathrm{S}^\mathrm{qu}}{\mathrm{d}\lambda^2}(0) + \mathcal{O}\left(\lambda^4\right). \tag{F35}$$

If we now do a Taylor series expansion of $\tau_\mathrm{MF}(\lambda)$ we find, using $\tilde{Z}_\mathrm{S}^\mathrm{qu}(0) = 1$,

$$\begin{aligned}
\tau_\mathrm{MF}(\lambda) &= \tau_\mathrm{S} + \tfrac{1}{2}\lambda^2 \left(\frac{\mathrm{d}^2\tilde{\rho}}{\mathrm{d}\lambda^2}(0) - \frac{\mathrm{d}^2\tilde{Z}_\mathrm{S}^\mathrm{qu}}{\mathrm{d}\lambda^2}(0)\tau_\mathrm{S}\right) + \mathcal{O}(\lambda^4) \\
&= \tau_\mathrm{S} + \lambda^2 \sum_n [[X_n^\dagger, \tau_\mathrm{S} X_n] A'_\beta(\omega_n) + \beta\tau_\mathrm{S}(X_n X_n^\dagger - \mathrm{tr}[\tau_\mathrm{S} X_n X_n^\dagger]) A_\beta(\omega_n)] \\
&\quad + \sum_{m\neq n} ([X_m, X_n^\dagger \tau_\mathrm{S}] + [\tau_\mathrm{S} X_n, X_m^\dagger]) \frac{A_\beta(\omega_n)}{\omega_{nm}} + \mathcal{O}(\lambda^4).
\end{aligned} \tag{F36}$$

We regain the expressions found in [32], but without having to consider any restrictions on β. In contrast, the binomial expansion based derivation of [32] seems to imply that irrespective of the choice of coupling strength, there will always be a temperature below which the binomial approximation will fail and (F36) can lead to incorrect results below this temperature. But this argument cannot be sustained as the validity of the

second order expansion is not constrained by any lower temperature limit implied by the binomial expansion as it can be obtained without making this approximation.

What we now have is the necessary requirement that (for some definition of the norm $||\dots||$ of the operators involved)

$$\tfrac{1}{2}\lambda^2\left|\left|\left(\frac{\mathrm{d}^2\tau_{\mathrm{MF}}}{\mathrm{d}\lambda^2}(0)-\tau_{\mathrm{S}}\frac{\mathrm{d}^2\tilde{Z}_{\mathrm{S}}^{\mathrm{qu}}}{\mathrm{d}\lambda^2}(0)\right)\right|\right|\ll||\tau_{\mathrm{S}}||, \tag{F37}$$

for the second order result (F36) to be valid. This of course is not a sufficient condition as the higher order terms, $\mathcal{O}(\lambda^4)$, are not guaranteed to be negligible.

The concern is the low temperature limit $\beta\to\infty$, where the term linear in β seems to imply linear divergence so the condition (F37) cannot be met. However, it can be shown that in this limit the second order correction term in (F36) actually vanishes [32]. It also does so for $\beta\to 0$, the high temperature limit, so there might be an intermediate temperature for which the condition (F37) is not satisfied, this then requiring a weaker interaction coupling strength.

The conclusion then is that for sufficiently weak coupling, the result (F36) will hold true for all temperatures.

To evaluate the second order expression for the normalised density operator given by (F36) we need to expand $X=S_\theta$ in terms of the energy eigenoperators X_n,

$$X=S_z\cos\theta-S_x\sin\theta=-\tfrac{1}{2}\sin\theta S_-+\cos\theta S_z--\tfrac{1}{2}\sin\theta S_+, \tag{F38}$$

so we can identify, from $X=X_{-1}+X_0+X_{+1}$,

$$X_{-1}=-\tfrac{1}{2}\sin\theta S_-, \tag{F39}$$
$$X_0=\cos\theta S_z, \tag{F40}$$
$$X_{+1}=-\tfrac{1}{2}\sin\theta S_+. \tag{F41}$$

To determine the corresponding eigenfrequencies, we use $[H_{\mathrm{S}},X_n]=\omega_n X_n$ and find that

$$[H_{\mathrm{S}},X_{-1}]=\left[-\omega_L S_z,-\tfrac{1}{2}\sin\theta S_-\right]=\omega_{\mathrm{L}}X_{-1}, \tag{F42}$$

and hence $\omega_{-1}=\omega_{\mathrm{L}}$. It follows that $\omega_{+1}=-\omega_{\mathrm{L}}$, and by inspection, $\omega_0=0$.

To evaluate $\tau_{\mathrm{MF}}^{(2)}$ we then have a number of sums to evaluate, and from that expression we can then calculate the expectation values of S_z and S_x. The calculation of these quantities is made 'easier' by the fact that τ_{S} is diagonal in the S_z basis, and that $\langle S_y\rangle=0$. After somewhat lengthy but straightforward calculations we find that

$$\begin{aligned}\langle S_z\rangle^{(2)}=\langle S_z\rangle_0&+\tfrac{1}{4}\hbar\lambda^2\sin^2\theta[(S_0(S_0+\hbar)-\langle S_z^2\rangle_0)\Sigma'(\omega_{\mathrm{L}})-\langle S_z\rangle_0\hbar\Delta'_\beta(\omega_{\mathrm{L}})]\\&-\beta\lambda^2[\tfrac{1}{4}\sin^2\theta((\langle S_z^2\rangle_0-\langle S_z\rangle_0^2)\hbar\Delta_\beta(\omega_{\mathrm{L}})+(\langle S_z^3\rangle_0-\langle S_z\rangle_0\langle S_z^2\rangle_0)\Sigma(\omega_{\mathrm{L}}))\\&-\cos^2\theta(\langle S_z^3\rangle_0-\langle S_z\rangle_0\langle S_z^2\rangle_0)Q],\end{aligned} \tag{F43}$$

and

$$\langle S_x\rangle^{(2)}=\lambda^2\frac{\sin 2\theta}{4\omega_{\mathrm{L}}}[(S_0(S_0+\hbar)-\langle S_z^2\rangle_0)\Sigma(\omega_{\mathrm{L}})-\hbar\langle S_z\rangle_0\Delta_\beta(\omega_{\mathrm{L}})-4\langle S_z^2\rangle_0 Q], \tag{F44}$$

where $\langle\dots\rangle_0=\mathrm{tr}[\tau_{\mathrm{S}}\dots]$.

F.3. Quantum to classical limit for weak coupling

In what follows we explicitly verify the quantum to classical transition in the large spin limit presented in appendix D, using the quantum and classical weak coupling expressions found in the previous sections.

First, (F43), we have $\langle S_z\rangle$, regrouped to read

$$\begin{aligned}\langle S_z\rangle=\langle S_z\rangle_0+\tfrac{1}{4}\lambda^2\sin^2\theta[&(S_0(S_0+\hbar)-\langle S_z^2\rangle_0)\hbar\Sigma'-\langle S_z\rangle_0\hbar^2\Delta'_\beta-\beta((\langle S_z^2\rangle_0-\langle S_z\rangle_0^2)\hbar\Delta_\beta\\&+(\langle S_z^3\rangle_0-\langle S_z\rangle_0\langle S_z^2\rangle_0)(\Sigma-2Q))]+\tfrac{1}{4}\beta\lambda^2(1+3\cos 2\theta)Q(\langle S_z^3\rangle_0-\langle S_z\rangle_0\langle S_z^2\rangle_0).\end{aligned} \tag{F45}$$

Introducing the scaled temperature $\beta' = \beta S_0$ and the scaled spin $s_z = S_z/S_0$ and taking the limit $S_0 \to \infty$ with β' held constant gives

$$\langle s_z\rangle = \langle s_z\rangle_0 + \tfrac{1}{4}\lambda^2\sin^2\theta[(1-\langle s_z^2\rangle_0)\hbar(S_0\Sigma') - \langle s_z\rangle_0\hbar^2\Delta'_\beta - \beta'((\langle s_z^2\rangle_0 - \langle s_z\rangle_0^2)\hbar\Delta_\beta + (\langle s_z^3\rangle_0 - \langle s_z\rangle_0\langle s_z^2\rangle_0)((S_0\Sigma) - 2S_0Q))] + \tfrac{1}{4}\beta'\lambda^2(1+3\cos 2\theta)(S_0Q)(\langle s_z^3\rangle_0 - \langle s_z\rangle_0\langle s_z^2\rangle_0). \tag{F46}$$

with (and noting that $S_0 J_\omega$ is independent of S_0)

$$S_0\Sigma \to \int_0^\infty (S_0J_\omega)\,\frac{2\omega}{\omega^2-\omega_{\rm L}^2}\,{\rm d}\omega, \tag{F47}$$

$$\Delta_\beta \to \int_0^\infty \frac{(S_0J_\omega)}{\hbar}\,\frac{4\omega_{\rm L}}{\omega^2-\omega_{\rm L}^2}\,\frac{1}{\beta'\omega}\,{\rm d}\omega, \tag{F48}$$

$$\Delta'_\beta \to \int_0^\infty \frac{(S_0J_\omega)}{\hbar^2}\,\frac{4\left(\omega^2+\omega_{\rm L}^2\right)}{\left(\omega^2-\omega_{\rm L}^2\right)^2}\,\frac{1}{\beta'\omega}\,{\rm d}\omega, \tag{F49}$$

$$S_0\Sigma' \to \int_0^\infty \frac{(S_0J_\omega)}{\hbar}\,\frac{4\omega_{\rm L}\omega}{\left(\omega^2-\omega_{\rm L}^2\right)^2}\,{\rm d}\omega, \tag{F50}$$

$$S_0Q \to \int_0^\infty (S_0J_\omega)\,\frac{1}{\omega}\,{\rm d}\omega. \tag{F51}$$

Making use of the $S_0 \to \infty$ limit of $\langle s_z^n\rangle_0$, $n = 1,2,3$ with β' held constant, given from (F20) by the classical forms (F7):

$$\langle s_z\rangle_0 = \coth(\beta'\omega_{\rm L}) - \frac{1}{\beta'\omega_{\rm L}}, \tag{F52}$$

$$\langle s_z^2\rangle_0 = 1 - \frac{2\coth(\beta'\omega_{\rm L})}{\beta'\omega_{\rm L}} + \frac{2}{(\beta'\omega_{\rm L})^2}, \tag{F53}$$

$$\langle s_z^3\rangle_0 = \coth(\beta'\omega_{\rm L}) - \frac{3}{\beta'\omega_{\rm L}} + \frac{6\coth(\beta'\omega_{\rm L})}{(\beta'\omega_{\rm L})^2} - \frac{6}{(\beta'\omega_{\rm L})^3}, \tag{F54}$$

and the above limiting forms for the integrals, we find that the factor multiplying $\sin^2\theta$ vanishes and we are left with

$$\langle s_z\rangle = \langle s_z\rangle_0 + \frac{1}{4}\beta'\lambda^2 S_0Q(1+3\cos 2\theta)\left(\langle s_z^3\rangle_0 - \langle s_z\rangle_0\langle s_z^2\rangle_0\right), \tag{F55}$$

which on substituting for the $\langle s_z^n\rangle_0$ yields a result formally identical to the fully classical result, (F13). In a similar way we can check the large spin limit for $\langle S_x\rangle$, and we regain the classical result, (F15).

Appendix G. Ultrastrong coupling limit

In this section the we examine ultrastrong coupling limit of the quantum and classical MF.

G.1. Classical ultrastrong coupling limit

The ultrastrong limit is the limit in which the coupling λ is made very large, in principle taken to infinity. To take this limit, first note that the partition function can be written as

$$Z_{\rm S}^{\rm cl} = Z_0^{\rm cl}\int_0^\pi {\rm d}\theta'\sin\theta' {\rm e}^{\beta\omega_L S_0\cos\theta'}F(\lambda,\theta,\theta'), \tag{G1}$$

where

$$F(\lambda,\theta,\theta') = \int_0^{2\pi}{\rm d}\varphi' {\rm e}^{\frac{1}{2}\beta\lambda^2 S_0^2 Q\left(\sin\theta\sin\theta'\cos\varphi' - \cos\theta\cos\theta'\right)^2}. \tag{G2}$$

Defining $a = \frac{1}{2}\beta Q S_0^2$, expanding the exponent and using the periodicity of the trigonometric functions we can rewrite

$$F(\lambda,\theta,\theta') = \mathrm{e}^{a\lambda^2\cos^2(\theta'-\theta)}H(\cos\theta'\cos\theta)\int_0^{2\pi}\mathrm{d}\varphi' \times \mathrm{e}^{-4a\lambda^2\sin\theta\sin\theta'\cos^2(\varphi'/2)(\sin\theta\sin\theta'\sin^2(\varphi'/2)+\cos\theta\cos\theta')} + \mathrm{e}^{a\lambda^2\cos^2(\theta'+\theta)}H(-\cos\theta'\cos\theta)\int_{-\pi}^{\pi}\mathrm{d}\varphi' \times \mathrm{e}^{-4a\lambda^2\sin\theta\sin\theta'\sin^2(\varphi'/2)(\sin\theta\sin\theta'\cos^2(\varphi'/2)-\cos\theta\cos\theta')} \tag{G3}$$

where $H(x)$ is the Heaviside step function. The advantage of this rewriting of $F(\lambda,\theta,\theta')$ is that now the exponents in the integrands are all negative (or zero) over the range of integration. The exponent of the integrand for the first integral where $\cos\theta'\cos\theta > 0$ will vanish at $\varphi' = \pi$, while for the second integral, where $\cos\theta'\cos\theta < 0$, the exponent of the integrand will vanish at $\varphi' = 0, 2\pi$. At these points the integrands will have local maxima which will become increasingly sharp as λ is increased. Similarly, for the second integral the maximum of the second integrand lies at $\varphi' = 0$.

Thus, as λ is increased, we can approximate the exponent in the integral by its behaviour in the neighbourhood of $\varphi' = \pi$ for the first integral, and in the neighbourhood of $\varphi' = 0$ for the second one. This is just using the method of steepest descent. We then obtain

$$Z_{\mathrm{S}}^{\mathrm{cl}} \sim Z_0^{\mathrm{cl}}\mathrm{e}^{a\lambda^2}\int_0^{\pi}\mathrm{d}\theta'\sin\theta'\mathrm{e}^{\beta\omega_{\mathrm{L}}S_0\cos\theta'}\left[\mathrm{e}^{-a\lambda^2\sin^2(\theta'-\theta)}R_-(\theta',\theta)H(\cos\theta'\cos\theta) \times \int_0^{2\pi}\mathrm{d}\varphi'\delta(\varphi'-\pi) + \mathrm{e}^{-a\lambda^2\sin^2(\theta'+\theta)}R_+(\theta',\theta)H(-\cos\theta'\cos\theta)\int_{-\pi}^{\pi}\mathrm{d}\varphi'\delta(\varphi')\right]. \tag{G4}$$

where

$$R_\pm(\theta',\theta) = \sqrt{\frac{\pi}{a\lambda^2|\sin\theta'\sin\theta\cos(\theta'\pm\theta)|}}, \tag{G5}$$

and for later interpretation purposes, the φ' integrals have been retained unevaluated.

Once again we notice that the exponents in the integrands are all negative. The zeroes of the exponents will occur within the range of integration for $\theta' = \theta$ for the first exponents, and for $\theta' = \pi - \theta$ for the second. Therefore, in the large λ limit we have

$$Z_{\mathrm{S}}^{\mathrm{cl}} \to \tilde{Z}_{\mathrm{S,US}}^{\mathrm{cl}} \sim Z_0^{\mathrm{cl}}\frac{\pi\,\mathrm{e}^{a\lambda^2}}{a\lambda^2}\int_0^{\pi}\mathrm{d}\theta'\mathrm{e}^{\beta\omega_L S_0\cos\theta'}\left[\int_0^{2\pi}\mathrm{d}\varphi'\delta(\theta'-\theta)\delta(\varphi'-\pi) + \int_{-\pi}^{\pi}\mathrm{d}\varphi'\delta(\theta'+\theta-\pi)\delta(\varphi')\right]. \tag{G6}$$

This suggests that in the large λ limit, the spin orients itself in either the $\theta' = \theta, \varphi' = \pi$ or $\theta' = \pi - \theta, \varphi' = 0$ directions, though with different weightings for the two directions.

If we return to the interaction on which this result is based, that is

$$V = (S_z\cos\theta - S_x\sin\theta)B = \mathbf{S}\cdot B(-\sin\theta\mathbf{x} + \cos\theta\mathbf{z}) = \mathbf{S}\cdot\mathbf{B}, \tag{G7}$$

we see that the vector $-\sin\theta\mathbf{x} + \cos\theta\mathbf{z}$ has the polar angles $\theta' = \theta, \varphi' = \pi$. But as B can be fluctuate between positive or negative values, the vector $\mathbf{B}$ can fluctuate between this and the opposite direction $\theta' = \pi - \theta, \varphi' = 0$. So the effect of the ultrastrong noise is to force the spin to orient itself in either of these two directions.

Returning to the expression for the partition function, we have

$$\tilde{Z}_{\mathrm{S,US}}^{\mathrm{cl}} \sim Z_0''\left(\mathrm{e}^{\beta\omega_L S_0\cos\theta} + \mathrm{e}^{-\beta\omega_L S_0\cos\theta}\right) \propto \cosh(\beta\omega_L S_0\cos\theta), \tag{G8}$$

where extraneous factors have been absorbed into Z_0''. These results are of the same form as found for a quantum spin half. That result is understandable given that the spin half would have two orientations, which mirrors the two orientations that emerge in the strong coupling limit here in the classical case.

G.2. Quantum ultrastrong coupling limit

The aim here is to derive an expression for the quantum MFG state of a spin S_0 particle coupled to a thermal reservoir at a temperature β^{-1}, (F16).

The ultrastrong coupling limit is achieved by making λ very much greater than all other energy parameters of the system, in effect, $\lambda \to \infty$. However, note the absence of the 'counter-term' $-\lambda^2(\cos\theta S_z - \sin\theta S_x)^2 Q$ in the above Hamiltonian. This term appears in [32], where it is found to be

cancelled in the strong coupling limit when the trace over the reservoir states is made. Here, that cancellation will not take place, so its presence must be taken into account. It will have no impact in the case of $S_0 = \frac{1}{2}$, as this will be a c-number contribution, but it will have an impact otherwise.

With $H_S = -\omega_L S_z$ and $P_{s_\theta} = |s_\theta\rangle\langle S_\theta|$ the projector onto the eigenstate $|s_\theta\rangle$ of S_θ where

$$S_\theta = \cos\theta S_z - \sin\theta S_x; \quad S_\theta|s_\theta\rangle = s_\theta|s_\theta\rangle \tag{G9}$$

we have, in the ultrastrong coupling limit, the unnormalised MFG state of the particle

$$\tilde{\rho} = \exp\left[-\beta \sum_{s_\theta=-S_0}^{S_0} P_{s_\theta} H_S P_{s_\theta}\right] \mathrm{e}^{\beta\lambda^2 S_\theta^2 Q} = \sum_{s_\theta=-S_0}^{S_0} P_{s_\theta} \exp\left[-\beta\langle s_\theta|H_S|s_\theta\rangle\right] \mathrm{e}^{\beta\lambda^2\gamma^2 s_\theta^2 Q}. \tag{G10}$$

Note, as a consequence of the absence of a counter-term, the contribution $\exp[\beta\lambda^2 S_\theta^2 Q]$ is not cancelled.

Further note the limits on the sum are $\pm S_0$. This follows since $S_\theta = \cos\theta S_z - \sin\theta S_x$ is just S_z rotated around the y axis, i.e.

$$\cos\theta S_z - \sin\theta S_x = \mathrm{e}^{\mathrm{i}\theta S_y} S_z \mathrm{e}^{-\mathrm{i}\theta S_y} = S_\theta \tag{G11}$$

so the eigenvalue spectrum of S_θ will be the same as that of S_z, i.e. $s_z = -S_0, -S_0+1, \ldots, S_0-1, S_0$. The eigenvectors of S_θ are then, from $S_z|s_z\rangle = s_z|s_z\rangle$

$$S_\theta \mathrm{e}^{\mathrm{i}\theta S_y}|s_z\rangle = s_z \mathrm{e}^{\mathrm{i}\theta S_y}|s_z\rangle \tag{G12}$$

i.e. the eigenvectors of S_θ are

$$|s_\theta\rangle = \mathrm{e}^{\mathrm{i}\theta S_y}|s_z\rangle; \quad s_\theta = s_z = -S_0, \ldots, S_0. \tag{G13}$$

We then have

$$\begin{aligned}\langle s_\theta|H_S|s_\theta\rangle &= \omega_L \langle s_z|\mathrm{e}^{-\mathrm{i}\theta S_y} S_z \mathrm{e}^{\mathrm{i}\theta S_y}|s_z\rangle \\ &= \omega_L \langle s_z|\cos\theta S_z + \sin\theta S_x|s_z\rangle \\ &= \omega_L s_z \cos\theta,\end{aligned} \tag{G14}$$

from which follows

$$\tilde{\rho} = \sum_{s_z=-S_0}^{S_0} \mathrm{e}^{\mathrm{i}\theta S_y}|s_z\rangle\langle s_z|\mathrm{e}^{-\mathrm{i}\theta S_y} \mathrm{e}^{\beta\omega_L S_z\cos\theta} \mathrm{e}^{\beta\lambda^2 Q s_z^2}. \tag{G15}$$

The partition function is then given by

$$\tilde{Z}_S^{\mathrm{qu}} = \sum_{s_z=-S_0}^{s_z=S_0} \mathrm{e}^{\beta\omega_L S_z\cos\theta} \mathrm{e}^{\beta\lambda^2 Q s_z^2}. \tag{G16}$$

This cannot be evaluated exactly, but the limit of large λ is yet to be taken. The dominant contribution to the sum in that limit will be for $s_z = \pm S_0$, so we can write

$$\tilde{Z}_{S,US}^{\mathrm{qu}} \mathrm{e}^{-\beta\lambda^2 Q S_0^2} \sim \mathrm{e}^{\beta\omega_L S_0\cos\theta} + \mathrm{e}^{-\beta\omega_L S_0\cos\theta} \propto \cosh\left(\beta\omega_L S_0\cos\theta\right). \tag{G17}$$

Apart from an unimportant proportionality factor, this is exactly the same results as found for the classical case in the limit of ultrastrong coupling, (G8).

ORCID iDs

F Cerisola https://orcid.org/0000-0003-2961-739X
S Scali https://orcid.org/0000-0002-8133-1551
J Anders https://orcid.org/0000-0002-9791-0363

References

[1] Bohr N 1920 *Z. Phys.* **2** 423
[2] Millard K and Leff H S 1971 *J. Math. Phys.* **12** 1000
[3] Lieb E H 1973 *Commun. Math. Phys.* **31** 327
[4] Liboff R L 1975 *Found. Phys.* **5** 271–93
[5] Liboff R L 1984 *Phys. Today* **37** 50–55
[6] Kryvohuz M and Cao J 2005 *Phys. Rev. Lett.* **95** 180405
[7] Graefe E-M, Korsch H J and Niederle A E 2010 *Phys. Rev.* A **82** 013629
[8] Jarzynski C, Quan H T and Rahav S 2015 *Phys. Rev.* X **5** 031038
[9] Chen J-F, Qiu T and Quan H-T 2021 *Entropy* **23** 1602
[10] Evans R F L, Fan W J, Chureemart P, Ostler T A, Ellis M O A and Chantrell R W 2014 *J. Phys.: Condens. Matter* **26** 103202
[11] Barker J and Bauer G E W 2019 *Phys. Rev.* B **100** 140401
[12] Strungaru M, Ellis M O A, Ruta S, Chubykalo-Fesenko O, Evans R F L and Chantrell R W 2021 *Phys. Rev.* B **103** 024429
[13] Barker J and Atxitia U 2021 *J. Phys. Soc. Japan* **90** 081001
[14] Vorndamme P, Schmidt H-J, Schröder C and Schnack J 2021 *New J. Phys.* **23** 083038
[15] Jarzynski C 2004 *J. Stat. Mech.* 09005
[16] Seifert U 2016 *Phys. Rev. Lett.* **116** 020601
[17] Jarzynski C 2017 *Phys. Rev.* X **7** 011008
[18] Strasberg P and Esposito M 2017 *Phys. Rev.* E **95** 062101
[19] Miller H J D and Anders J 2017 *Phys. Rev.* E **95** 062123
[20] Aurell E 2018 *Phys. Rev.* E **97** 042112
[21] Mori T and Miyashita S 2008 *J. Phys. Soc. Japan* **77** 124005
[22] Campisi M, Talkner P and Hänggi P 2009 *J. Phys. A: Math. Theor.* **42** 392002
[23] Hilt S, Shabbir S, Anders J and Lutz E 2011 *Phys. Rev.* E **83** 030102
[24] Fleming C H and Cummings N I 2011 *Phys. Rev.* E **83** 031117
[25] Thingna J, Wang J-S and Hänggi P 2012 *J. Chem. Phys.* **136** 194110
[26] Subaşi Y, Fleming C H, Taylor J M and Hu B L 2012 *Phys. Rev.* E **86** 061132
[27] Philbin T G and Anders J 2016 *J. Phys. A: Math. Theor.* **49** 215303
[28] Miller H J D and Anders J 2018 *Nat. Commun.* **9** 2203
[29] Strasberg P 2019 *Phys. Rev. Lett.* **123** 180604
[30] Trushechkin A 2021 arXiv:2109.01888
[31] Trushechkin A S, Merkli M, Cresser J D and Anders J 2022 *AVS Quantum Sci.* **4** 012301
[32] Cresser J D and Anders J 2021 *Phys. Rev. Lett.* **127** 250601
[33] Ferialdi L 2017 *Phys. Rev.* A **95** 020101
[34] Chiu Y-F, Strathearn A and Keeling J 2021 arXiv:2112.08254 [quant-ph]
[35] Trushechkin A 2019 *J. Chem. Phys.* **151** 074101
[36] Yang M and Fleming G R 2002 *Chem. Phys.* **282** 163
[37] Kolli A, O'Reilly E J, Scholes G D and Olaya-Castro A 2012 *J. Chem. Phys.* **137** 174109
[38] Moix J M, Zhao Y and Cao J 2012 *Phys. Rev.* B **85** 115412
[39] Huelga S and Plenio M 2013 *Contemp. Phys.* **54** 181
[40] Seibt J and Mančal T 2017 *J. Chem. Phys.* **146** 174109
[41] Gelzinis A and Valkunas L 2020 *J. Chem. Phys.* **152** 051103
[42] Purkayastha A, Guarnieri G, Mitchison M T, Filip R and Goold J 2020 *npj Quantum Inf.* **6** 27
[43] Anders J, Sait C R J and Horsley S A R 2022 *New J. Phys.* **24** 033020
[44] Unikandanunni V, Medapalli R, Asa M, Albisetti E, Petti D, Bertacco R, Fullerton E E and Bonetti S 2022 *Phys. Rev. Lett.* **129** 237201
[45] Neeraj K *et al* 2021 *Nat. Phys.* **17** 245
[46] Neeraj K, Pancaldi M, Scalera V, Perna S, d'Aquino M, Serpico C and Bonetti S 2022 *Phys. Rev.* B **105** 054415
[47] Stupakiewicz A, Davies C, Szerenos K, Afanasiev D, Rabinovich K, Boris A, Caviglia A, Kimel A and Kirilyuk A 2021 *Nat. Phys.* **17** 489
[48] Nazir A 2009 *Phys. Rev. Lett.* **103** 146404
[49] Recati A, Fedichev P O, Zwerger W, von Delft J and Zoller P 2005 *Phys. Rev. Lett.* **94** 040404
[50] Magazzù L, Forn-Díaz P, Belyansky R, Orgiazzi J-L, Yurtalan M A, Otto M R, Lupascu A, Wilson C M and Grifoni M 2018 *Nat. Commun.* **9** 1403
[51] Popovic M, Mitchison M T, Strathearn A, Lovett B W, Goold J and Eastham P R 2021 *PRX Quantum* **2** 020338
[52] Breuer H-P and Petruccione F 2007 *The Theory of Open Quantum Systems* (Oxford University Press)
[53] Huttner B and Barnett S M 1992 *Phys. Rev.* A **46** 4306
[54] Fruchtman A, Lambert N and Gauger E M 2016 *Sci. Rep.* **6** 2045
[55] Wu J, Liu F, Shen Y, Cao J and Silbey R J 2010 *New J. Phys.* **12** 105012
[56] Ritschel G, Roden J, Strunz W T and Eisfeld A 2011 *New J. Phys.* **13** 113034
[57] Scali S, Horsley S, Anders J and Cerisola F 2023 Spidy.jl – open-source Julia package for the study of non-Markovian stochastic dynamics (arXiv:2310.03008 [physics.comp-ph])
[58] Latune C L 2021 arXiv:2110.02186 [quant-ph]
[59] Jakšić V and Pillet C-A 1996 *Commun. Math. Phys.* **178** 627
[60] Merkli M 2001 *Commun. Math. Phys.* **223** 327
[61] Bach V, Fröhlich J and Sigal I M 2000 *J. Math. Phys.* **41** 3985
[62] Merkli M 2021 Correlation decay and markovianity in open systems (arXiv:2107.02515)
[63] Merkli M 2022 *Quantum* **6** 615
[64] Merkli M 2022 *Quantum* **6** 616
[65] Fisher M E 1964 *Am. J. Phys.* **32** 343
[66] Wang Y K and Hioe F T 1973 *Phys. Rev.* A **7** 831
[67] Campisi M, Talkner P and Hänggi P 2009 *Phys. Rev. Lett.* **102** 210401
[68] Strasberg P and Esposito M 2020 *Phys. Rev.* E **101** 050101

[69] Nemati S, Henkel C and Anders J 2021 arXiv:2112.04001 [quant-ph]
[70] Latune C L 2022 *Phys. Rev.* E **105** 024126
[71] Iles-Smith J, Lambert N and Nazir A 2014 *Phys. Rev.* A **90** 032114
[72] Iles-Smith J, Dijkstra A G, Lambert N and Nazir A 2016 *J. Chem. Phys.* **144** 044110
[73] Nazir A and Schaller G 2018 The reaction coordinate mapping in quantum thermodynamics *Thermodynamics in the Quantum Regime: Fundamental Aspects and New Directions* ed F Binder, L A Correa, C Gogolin, J Anders and G Adesso (Springer International Publishing) pp 551–77
[74] Correa L A, Xu B, Morris B and Adesso G 2019 *J. Chem. Phys.* **151** 094107
[75] Auffèves A 2022 *PRX Quantum* **3** 020101
[76] Anto-Sztrikacs N, Nazir A and Segal D 2022 arXiv:2211.05701
[77] Hogg C R, Cerisola F, Cresser J D, Horsley S A R and Anders J 2023 Enhanced entanglement in multi-bath spin-boson models (arXiv:2306.11036 [quant-ph])
[78] Hartmann F, Scali S and Anders J 2023 *Phys. Rev.* B **108** 184402
[79] Berritta M, Scali S, Cerisola F and Anders J 2023 Accounting for quantum effects in atomistic spin dynamics (arXiv:2305.17082 [cond-mat.mtrl-sci])